PHYSICAL REVIEW B VOLUME 20, NUMBER 8 15 OCTOBER 1979

Descriptions of exchange and correlation effects in inhomogeneous electron systems

O. Gunnarsson
Institut für Festkörperforschung der Kernforschungsanlage Jülich, D-5170 Jülich, Germany

M. Jonson*
Institute of Theoretical Physics, Chalmers University of Technology, S-41296 Göteborg, Sweden

B. I. Lundqvist†
Institute of Physics, University of Aarhus, DK-8000 Aarhus, Denmark
(Received 27 November 1978)

Starting from a formula relating the exchange-correlation (XC) energy of the Kohn-Sham density-functional formalism to the XC hole, we discuss some general but approximate descriptions of XC effects in inhomogeneous electron systems, in particular valence electrons, using homogeneous-electron-gas data as input. The new descriptions have all the virtues of the local-density (LD) approximation, including the computational simplicity of a local XC potential, and it reduces to the latter in the proper limit. In addition, they have a physically motivated nonlocal dependence on the electron density, which results in such desirable features as an asymptotical r^{-1} behavior far away from, e.g., atoms and a z^{-1} behavior of the potential outside solid surfaces. We present two explicit forms of the XC energy functional, one which is exact for a system with almost constant density but with possibly spatially rapid variations, and another which is exact in some simple limits. Illustrations on atoms show them to reduce the error in the total energy by about one order of magnitude compared with the LD approximation. Applications to surfaces show a reasonable modeling of the image-potential effect but also illustrate shortcomings of the approximations. We also point out shortcomings of two earlier methods to extend the LD approximation, the gradient expansion, and the expansion to second order in the density variations, when they are applied to inhomogeneous systems.

I. INTRODUCTION

A quantitative understanding of many-particle systems requires a knowledge of the correlations (or interactions) between the particles. A powerful and practical scheme to describe such correlation effects has been developed by Kohn and Sham[1] on the basis of the density-functional formalism of Hohenberg and Kohn.[2] The essence of the scheme is that the many-body problem is formulated within a single-particle framework, where the many-body nature of the problem enters via an exchange-correlation (XC) potential $v_{\rm XC}(\vec{r})$. This potential is defined as a functional derivative of an XC energy functional $E_{\rm XC}\{n\}$ of the density $n(\vec{r})$.

In view of the increasingly efficient and accurate methods to solve the Schrödinger equation, the central issue in the study of the electronic structure of atoms, molecules, and solids is the construction of the potential. In this perspective it is a virtue of the Kohn-Sham scheme to provide a basis for a single-particle potential $v_{\rm XC}(\vec{r})$ and for the functional

$$E_{\rm XC}\{n\}=\int n(r)\epsilon_{\rm XC}(\vec{r})\,d^3r\,,$$

where $\epsilon_{\rm XC}(r)$ is the XC energy density.

Another reason for the broad use of the Kohn-Sham scheme is that even a fairly crude approximation for the XC energy functional can give a good description of a large class of properties. To be specific, a local-density (LD) approximation

$$E_{\rm XC}\{n\}\approx\int n(\vec{r})\epsilon_{\rm XC}(n(\vec{r}))\,d^3r\,, \tag{1}$$

where $\epsilon_{\rm XC}(n)$ is the XC energy per electron of a homogeneous electron liquid with density n, has been employed in most applications of the scheme, in spite of the fact that the true XC interaction is manifestly *nonlocal*. This local approximation, generalized in order to describe spin polarizations, has provided a remarkably successful description of quite a number of atomic, molecular, and solid-state systems and properties.[3] For many of these systems, however, there is no *a priori* justification for using a LD approximation. In some applications, the LD approximation is known to give an insufficient accuracy and to fail to account for certain features; for instance, it gives exponentially decaying $\epsilon_{\rm XC}(\vec{r})$ and $v_{\rm XC}(\vec{r})$ for neutral atoms[4] and metal surfaces[5] rather than the proper power-law behavior, $-r^{-1}$ and $-1/4z$, respectively. Therefore, a considerable amount of activity has been devoted to *nonlocal* approximations to the XC energy functional.

One of the most used nonlocal approximations includes the lowest-order density-gradient corrections.[1,2,6] The XC energy functional is given by

$$E_{\rm XC}\{n\}\approx \int n(\vec{r})\epsilon_{\rm XC}(n(\vec{r}))\,d^3r + \int c(n(\vec{r}))\frac{|\nabla n(\vec{r})|^2}{n^{4/3}(\vec{r})}\,d^3r, \quad (2)$$

where $c(n(\vec{r}))$ is a function of the density. In the simple case of weak density variations, however, the gradient corrections do not seem to improve upon the LD approximation.[7] The expansion (2) is aimed at systems of slowly varying density, i.e., of the form $n(\vec{r})=\nu(\vec{r}/r_0)$ with $r_0\to\infty$, where $\nu(\vec{x})$ is a continuous function.

A different class of systems is characterized by an almost-constant density, i.e., $n(\vec{r})=n_0+\Delta n(\vec{r})$ with $|\Delta n(\vec{r})/n_0|\ll 1$ and n_0 constant. Summation of a subseries of gradient terms in this limit gives to the lowest order in Δn[1,2]

$$E_{\rm XC}\{n\}\approx \int n(\vec{r})\epsilon_{\rm XC}(n(\vec{r}))\,d^3r - \tfrac{1}{4}\int\int K_{\rm XC}(\vec{r}-\vec{r}',n) \times [n(\vec{r})-n(\vec{r}')]^2 d^3r\,d^3r', \quad (3)$$

where $K_{\rm XC}$ is directly related to the dielectric function of the homogeneous electron liquid of density n. The density parameter n in $K_{\rm XC}(\vec{r}-\vec{r}',n)$ is well defined in the proper limit of almost-constant density, where it is n_0. When Eq. (3) is used for inhomogeneous systems, however there are several plausible choices for the argument n, and we will show in Sec. II that this ambiguity leads to results ranging from finite to infinite values for XC energies of atoms and metal surfaces.

Neither of these nonlocal approximations seems to provide any systematic improvement on the local-density approximation for real physical systems. In order to successfully extend the LD approximation to include nonlocal effects, it is important to understand why, in practice, the local approximation works at all for systems with relatively rapid density variations. We believe the main reason to be that the LD approximation satisfies the criterion of charge conservation, starting that the XC hole should contain exactly one electron.[3]

In this paper we propose two approximations to the XC energy functional with nonlocal density dependence that retains this essential property: The first one, for later reference called the *average-density* (AD) *approximation*, is obtained by writing $E_{\rm XC}$ as

$$E_{\rm xc}\{n\}\approx \int n(\vec{r})\epsilon_{\rm XC}(\bar{n}(\vec{r}))\,d^3r. \quad (4)$$

The nonlocal-density dependence is introduced through $\bar{n}(\vec{r})$, which is a weighted average of the density in the neighborhood of the point $\vec{r}$. The weighting automatically corrects some of the exaggerations of the LD approximation [Eq. (1)], such as the magnitude of $\epsilon_{\rm XC}^{\rm LD}(\vec{r})$ for atoms being an overestimate close to the nucleus and an underestimate in the outskirts of the atom.[8] The weighting is obtained by requiring that Eq. (3) should be reproduced in the proper limit. Whereas the LD approximation is exact in the limit of almost-constant density with spatially slow variations, this prescription for $\bar{n}(\vec{r})$ makes the nonlocal approximation (4) exact in the limits of almost constant density *without any restrictions on the rapidness of the spatial variations.*

The second prescription, called the *weighted-density* (WD) *approximation*, is similar in spirit, in that it extends the LD approximation to one that depends on densities in a neighborhood. The weighting is different, however, and the details will be described in Sec. II.

It should be stressed that our main interest is the description of the valence electrons, due to their great importance for the behavior of molecules and solids. Further, the model system behind the functional for the description of the XC effects should be most appropriate for valence electrons or, more generally, for intrashell exchange and correlation. To avoid an inaccurate description of intershell effects, a scheme for subdivision of the density is proposed (Sec. III) and used (Sec. IV).

The input parameters for expansion (4), for the prescription for $\bar{n}(\vec{r})$ and for the WD approximation come from homogeneous-electron-liquid calculations. We give in this paper numerical results to be used as input in the prescriptions (Sec. III), and as illustrations of the methods, we apply them to the calculation of the total energy of a number of atoms (Sec. IV) and for some surface properties of metals in a simple model (Sec. V). These systems have been used in earlier studies of the LD approximation and attempts to improve it.

Compared with the LD approximation, the error in the exchange energy of a series of light atoms is reduced by almost one order of magnitude in both the AD and WD schemes. This essentially holds also for the XC energies in the AD scheme, whereas in this case the WD scheme hardly improves upon the results of the LD approximation. In addition, our methods model the $-r^{-1}$ behavior of $\epsilon_{\rm XC}(\vec{r})$ in the outskirts of a neutral atom and the z^{-1} behavior of the potential outside a metal surface. Unfortunately, the surface energies come out wrong in the two approximations, the AD result being much too large and the WD result being too small.

The virtues and the shortcomings of the AD and

WD approximations are summarized and discussed in Sec. VI.

II. FUNCTIONALS WITH A NONLOCAL-DENSITY DEPENDENCE

For later reference we give a few formulas of the density-functional formalism.[1] A basic quantity in this approach is the exchange-correlation energy functional $E_{\rm XC}\{n\}$, which is defined by

$$E_v\{n\} = T_0\{n\} + \int n(\vec{r}) v(\vec{r})\, d^3r + \frac{e^2}{2}\int \frac{n(\vec{r}) n(\vec{r}')}{|\vec{r}-\vec{r}'|}\, d^3r\, d^3r' + E_{\rm XC}\{n\}, \quad (5)$$

where $E_v\{n\}$ is the functional for the total energy of an interacting system with the density $n(\vec{r})$ in an external potential $v(\vec{r})$ and $T_0\{n\}$ is the functional for the kinetic energy of a noninteracting system with the same density. In this formalism the electron density is obtained from

$$n(\vec{r}) = \sum_{\nu}^{\rm occ} |\Psi_\nu(\vec{r})|^2, \quad (6)$$

where $\Psi_\nu(\vec{r})$ are solutions of a Schrödinger-like equation

$$[-\hbar^2\nabla^2/2m + v(\vec{r}) + V_H(\vec{r}) + v_{\rm xc}(\vec{r})]\,\Psi_\nu(\vec{r}) = \epsilon_\nu \Psi_\nu(\vec{r}). \quad (7)$$

The Hartree potential $V_H(\vec{r})$ is calculated from

$$V_H(\vec{r}) = e^2 \int \frac{n(\vec{r}')}{|\vec{r}-\vec{r}'|}\, d^3r', \quad (8)$$

and the XC potential $v_{\rm XC}(\vec{r})$ is defined

$$v_{\rm XC}(\vec{r}) = \delta E_{\rm XC}\{n\}/\delta n(\vec{r}). \quad (9)$$

The main problem in this approach is to determine $E_{\rm XC}\{n\}$. Once a functional form for $E_{\rm XC}\{n\}$ is assumed, Eqs. (6)–(9) can be solved self-consistently, giving the density of the system and through Eq. (5) the total energy. In this way ground-state properties of the system can be obtained.

We will first discuss the two approaches (2) and (3) to go beyond the local-density (LD) approximation (1) by using a nonlocal dependence on the density. In doing so we will point out some difficulties, and show the need for a new functional.

The gradient expansion[1,2] has in particular been applied to atoms, e.g., by Herman *et al.*[6] They pointed out that in this case the potential (9) is divergent both at the nucleus and in the density tail far from the nucleus. Therefore they introduced a convergence factor in the potential, which makes it finite over all space. However, Schwartz[9] has shown that the results are sensitive to the form of the convergence factor. The problem of a divergent $v_{\rm XC}$ in the tail region should be present also for metallic surfaces. In recent calculations[10,11] of the surface energy and work function, however, it has been avoided by using the method of potential variation,[12] which minimizes the energy functional directly,[10] or by using model densities in the functional.

Difficulties of the gradient expansion can also be illustrated by considering a simple system with an almost constant density but with possibly rapid variations, for which the expression (4) is correct. In this limit a gradient expansion is equivalent to a power expansion of the Fourier transform $K_{\rm xc}(q)$ of the kernel $K_{\rm XC}(r)$ in Eq. (3).[2] We shall therefore study the expansion of $K_{\rm XC}(q)$. In Fig. 1 we show the $K_{\rm XC}(q)$ obtained from the dielectric function calculated by Geldart and Taylor[13] together with the curves for the power expansions corresponding to the local-density approximation and the two lowest-order gradient corrections. For real physical systems the density has important Fourier components for wave vectors of the order of Fermi wave vectors. Fig. 1 shows important deviations in this range. It is questionable, if the first gradient correction gives any improvement of the LD approximation, and the second-lowest correction worsens the result drastically.

The expansion to second order in the density variations (3) is correct for weak but possibly

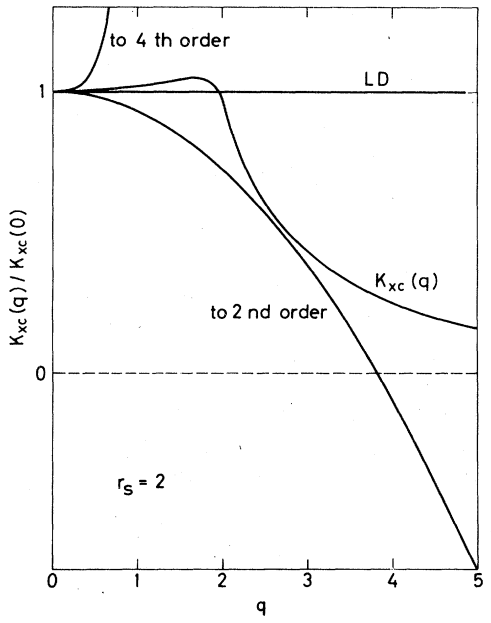

FIG. 1. Fourier transform of the kernel $K_{\rm XC}(r,n)$ in Eq. (3) for $r_s = 2$, compared with the results of using the local-density approximation (marked LD) and adding the lowest and two lowest-order gradient corrections, respectively ($q \equiv k/k_F$).

rapid variations. Equation (3) is thus derived[1,2] assuming that the density of the system is

$$n(\vec{r}) = n_0 + \Delta n(\vec{r}) , \tag{10}$$

with

$$\int \Delta n(\vec{r})\, d^3r = 0 . \tag{11}$$

Then the XC energy functional E_{XC} is expressed in terms of a kernel $K_{XC}(\vec{r}-\vec{r}', n_0)$, which is related to the dielectric function of a homogeneous medium with the density n_0 (see Appendix A). For extrapolations to real systems with strong density variations, however, the theory does not provide a satisfactory prescription for how to calculate the density argument n of Eq. (3). Hohenberg and Kohn[2] have suggested the form

$$n(\tfrac{1}{2}(\vec{r}+\vec{r}')) . \tag{12a}$$

A second plausible argument is

$$\tfrac{1}{2}[n(\vec{r}) + n(\vec{r}')] , \tag{12b}$$

but there are many other reasonable choices, for instance some weighted average of $n(\vec{r})$. Sham[14] proposed

$$n(\tfrac{1}{2}(|\vec{r}| + |\vec{r}'|)) \tag{12c}$$

for atoms, where $|\vec{r}|$ is the distance to the nucleus. All these forms would give the same result for a system with weak density variations. In the following we shall show, however, that for a real physical system the result is sensitive to the choice of the density argument, and that the lack of a theory on this point therefore is crucial.

We first present in Fig. 2 the integrand of Eq. (3) for bulk copper. The figure shows that the two density arguments (12a) and (12b) above give results that typically differ by one order of magnitude. This difference is due to the different ranges of the kernel in the two cases. The kernel becomes small if $rk_F(n) \gg 1$, where k_F is the Fermi wave vector. Assume that $\vec{r}$ is at the Wigner-Seitz radius and $\vec{r}'$ in the core region. As $\frac{1}{2}(\vec{r}+\vec{r}')$ then lies in the valence region, (12a) gives only a moderately large density argument. Although the kernel is small in this situation, it is not negligible and together with the very large factor $[n(\vec{r}) - n(\vec{r}')]^2$ it gives an important contribution. If, on the other hand, (12b) is used, the corresponding $k_F(\frac{1}{2}[n(\vec{r})+n(\vec{r}')])$ is so large that the kernel almost cuts off the contributions from the core region. To show that the discrepancy between (12a), (12b), and (12c) remains also after the integrations have been performed, we give in Appendixes A and B some results for atoms and surfaces.

In Appendix A we have applied the expression (3) to atoms. We find that using (12b) above, the XC energy is finite. On the other hand, application of (12a) or (12c) makes the integral in (3) divergent, i.e., the energy is infinite and positive.

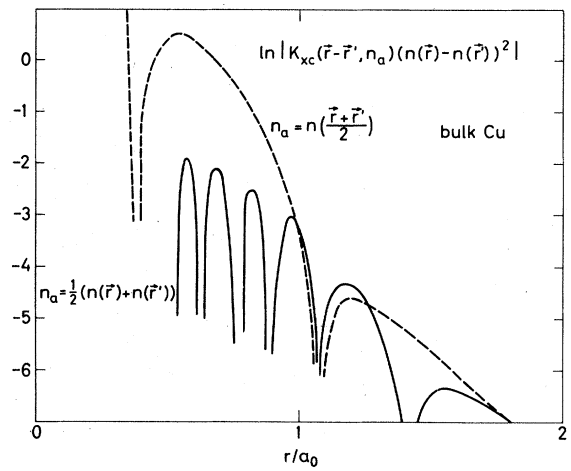

FIG. 2. Absolute value of the integrand of Eq. (3) for bulk copper. The vectors $\vec{r}$ and $\vec{r}'$ are assumed to be parallel and r is fixed at the Wigner-Seitz radius. The figure shows the difference between the choice (i) $n(\frac{1}{2}(\vec{r}+\vec{r}'))$ (dashed curve) and (ii) $\frac{1}{2}[n(\vec{r})+n(\vec{r}')]$ (full curve) for the density argument. Observe the logarithmic scale.

The application of Eq. (3) to a metal surface is discussed in Appendix B. Again, we find that (12b) gives a finite surface energy, while the energy is infinite if (12a) is used. It should be noted that for the gradient expansion the divergencies appear in the XC potential, while they occur already in the XC energy for the second-order expansion (3). In the latter case there is obviously no sensible way of using convergence factors, if one is interested in the energy of the system.

III. DERIVATION OF NEW NONLOCAL FUNCTIONALS

A. Exchange-correlation hole

The LD functional (1) and the gradient-corrected ones in Sec. II have been derived assuming slow density variations, i.e., for densities fulfilling the criteria[2]

$$|\nabla n(\vec{r})/n(\vec{r})| \ll k_F(n(\vec{r}))$$

and

$$|\nabla_i \nabla_j n(\vec{r})/\nabla n(\vec{r})| \ll k_F(n(\vec{r})) , \tag{13}$$

where $k_F(n) = (3\pi^2 n)^{1/3}$ is the "local" Fermi wave vector. Figure 3 shows that the density gradients of bulk Cu and for the jellium model of a metal surface ought to be about one order of magnitude smaller to make the use of these functionals well justified according to criterion (13). Considering

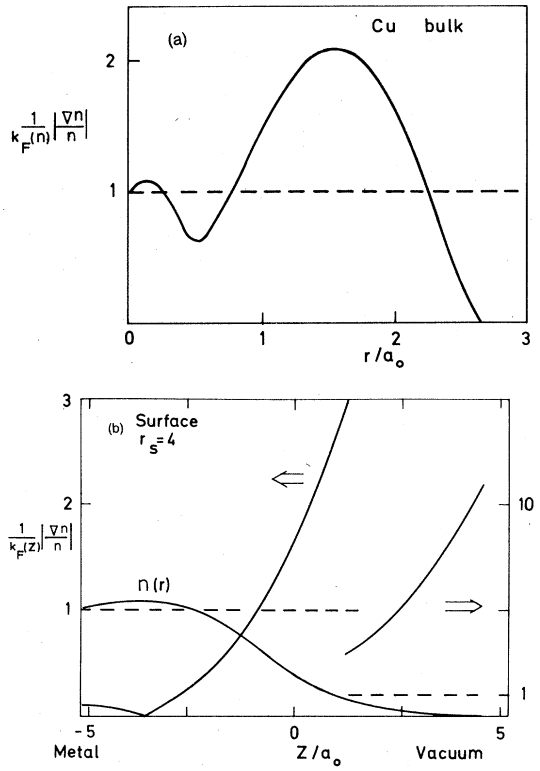

FIG. 3. (a) Typical values for the density gradient [Eq. (13)] in metallic copper as a function of the distance from the closest nucleus. (b) The same quantity in the jellium model for a surface. The z coordinate is perpendicular to the surface. The curve marked $n(r)$ shows the electron density.

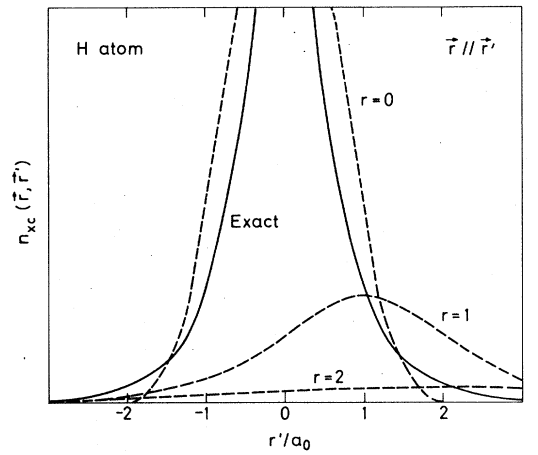

FIG. 4. Exchange-correlation hole $n_{\mathrm{XC}}(\vec{r},\vec{r}')$ (Eq. 15) for a hydrogen atom. The full curve shows the exact hole, while the dashed curves depict the hole in the LD approximation [Eq. (16)] for various positions of the electron (0, 1, and 2 a.u. from the proton), using the dielectric function of Singwi *et al* (Ref. 37). The x-axis gives the distance from the nucleus.

such rapid density variations, the failures of the nonlocal functionals discussed in Sec. II are not surprising.

On the other hand, the LD approximation has been successfully applied to a large number of systems and properties. This indicates that valuable features of the LD approximation have been lost in the generalization to these nonlocal functionals. In the rest of this section we will therefore discuss why the LD approximation is so successful and use this experience to construct new nonlocal functionals.

The XC energy can conveniently be viewed as the interaction between an electron and the charge $n_{\mathrm{XC}}(\vec{r},\vec{r}')$ of its XC hole. The hole describes how the probability of finding an electron at $\vec{r}'$, given an electron is present at $\vec{r}$, is suppressed due to the Pauli principle and the Coulomb interaction. An exact expression for the XC energy can be written[3,15]

$$E_{\mathrm{XC}}\{n\}=\frac{e^2}{2}\int d^3r\, n(\vec{r})\int d^3r'\,\frac{1}{|\vec{r}-\vec{r}'|}\,n_{\mathrm{XC}}(\vec{r},\vec{r}')\,, \tag{14}$$

with

$$n_{\mathrm{XC}}(\vec{r},\vec{r}')=n(\vec{r}')\int_0^1[g_n(\vec{r},\vec{r}';\lambda)-1]\,d\lambda \equiv n(\vec{r}')G(\vec{r},\vec{r}')\,, \tag{15}$$

where $g_n(\vec{r},\vec{r}';\lambda)$ is the pair correlation function of a system with a density $n(\vec{r})$ and the coupling constant λe^2. The density $n(\vec{r}')$ is evaluated for the physical value of λ ($\lambda=1$).[3] The LD approximation means that we use the pair correlation function $g^h_{n(\vec{r})}(\vec{r}-\vec{r}';\lambda)$ for the homogeneous electron liquid of density $n(\vec{r})$ and write

$$n^{\mathrm{LD}}_{\mathrm{XC}}(\vec{r},\vec{r}')\approx n(\vec{r})\int_0^1[g^h_{n(\vec{r})}(\vec{r}-\vec{r}';\lambda)-1]\,d\lambda\,. \tag{16}$$

Figure 4 shows the exact and the LD result for n_{XC} of a hydrogen atom, illustrating the drastic difference between the exact and the approximate holes. The former is centered on the proton and its size is independent of the electron position. The latter follows the electron and has a size, which varies strongly with the electron coordinate. Figure 5 gives an illustration for a many-electron atom, neon. To be able to compare with exact results, we have included only exchange effects, which makes the integral over λ in Eq. (16) trivial. The disagreement between the exact result and the LD approximation is not unexpected in view of the lacking formal justification for the LD approximation for inhomogeneous systems. That the LD approximation still can give good results, can be understood as follows[3]:

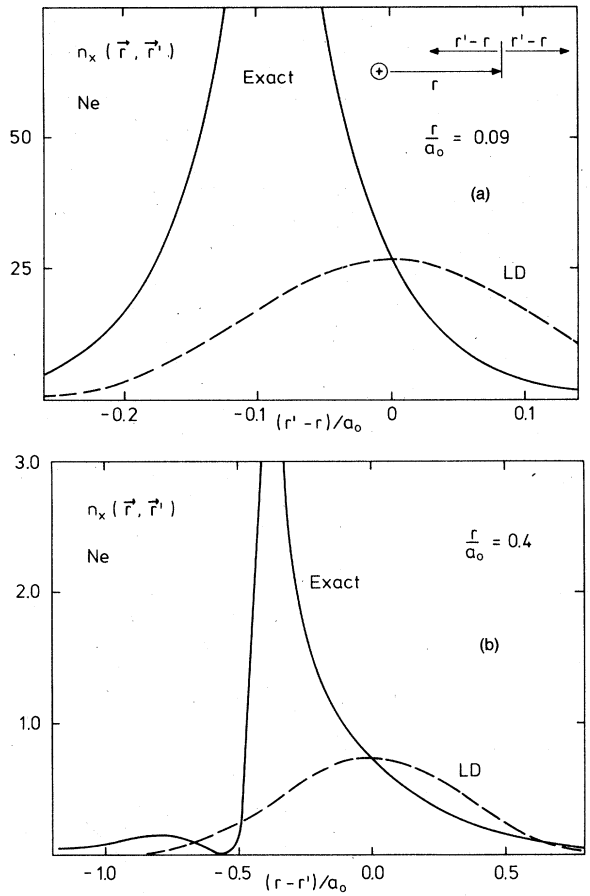

FIG. 5. Exchange hole $n_x(\vec{r},\vec{r}')$ for a neon atom. The full curves show exact results and the dashed curves show the results in the LD approximation. The curves in (a) and (b) are for two different values of r.

First, only the spherical average

$$n_{XC}^{SA}(\vec{r},r'') = (4\pi)^{-1}\int_{|\vec{r}-\vec{r}'|=\vec{r}''} d^3r'\, n_{XC}(\vec{r},\vec{r}')\,, \qquad (17)$$

of the hole influences the energy. Figure 6 shows

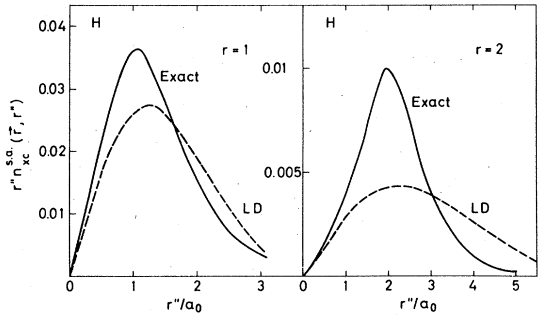

FIG. 6. Spherical average of the hydrogen XC hole [Eq. (16)] times r'' for $r=1$ and 2 a.u. as a function of r''. The full curves give the exact results and the dashed curves are calculated in the LD approximation.

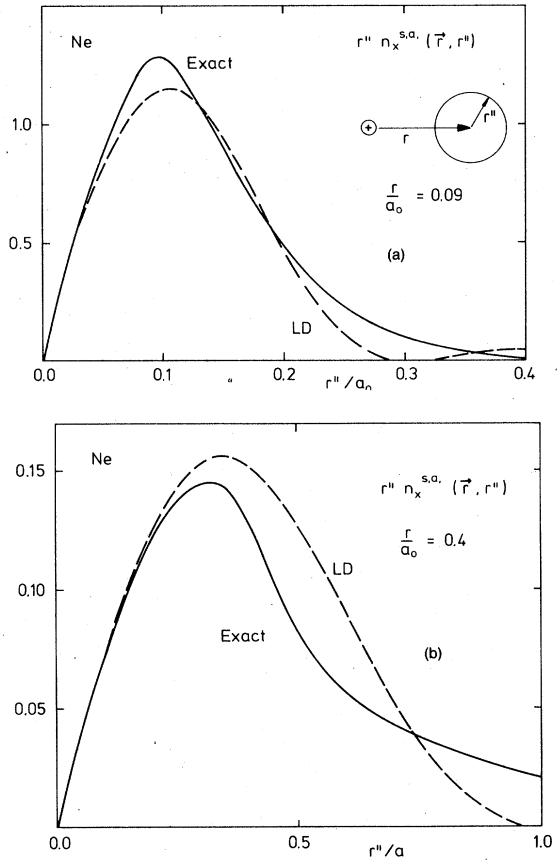

FIG. 7. Spherical average of the neon exchange hole [Eq. (17)] times r'' for (a) $r=0.09$ a. u. and (b) $r=0.4$ a.u. The full curves give the exact results and the dashed curves are obtained in the LD approximation.

this average for the hydrogen atom, with $|\vec{r}|=1$ and 2 a.u., and Fig. 7 is a similar plot for neon. It illustrates the partial cancellation of errors that will generally occur, when calculating the average.

Secondly, the LD approximation satisfies charge conservation. This can be expressed as a sum rule[3]

$$\int d^3r'\, n_{XC}(\vec{r},\vec{r}') = -1\,, \qquad (18a)$$

or

$$\int_0^\infty r''^2\, dr''\, n_{XC}^{SA}(\vec{r},r'') = -1\,, \qquad (18b)$$

stating that the XC hole corresponds to the removal of one electron charge. Equation (18b) implies that if $n_{XC}^{SA}(\vec{r},r'')$ has positive errors for some values of r'', it is bound to have negative errors for other values, implying a systematic partial cancellation of errors. This is illustrated for the hydrogen atom in Fig. 8, which shows the XC energy density

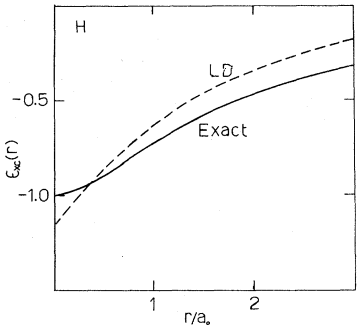

FIG. 8. Exchange-correlation energy density for hydrogen [Eq. (19)] as a function of the distance from the nucleus. The curves show the exact result and the result in the LD approximation, respectively.

[derived from Eqs. (14) and (17)]

$$\epsilon_{XC}(\vec{r}) = \tfrac{1}{2} e^2 \int_0^\infty r'' \, dr'' n_{XC}^{SA}(\vec{r}, r'') , \tag{19}$$

resulting after the r'' integration is performed. We note that for $|\vec{r}| = 2$ the error of typically a factor of 2 in $n_{XC}^{SA}(\vec{r}, r'')$ is reduced to about 30% for $\epsilon_{XC}(r)$. (The numerical results can be further improved by using a spin-dependent formalism.[8]) Figure 12(b) shows the corresponding result for neon. The conclusions of this analysis are therefore that in order to improve upon E_{XC}, (a) we should concentrate on improving the description of the spherical part n_{XC}^{SA} of the hole, as the nonspherical parts do not contribute to E_{XC}, and (b) the approximate functional should satisfy the sum-rule (18).

B. Average-density approximation

In looking for improved approximations, we observe that $n_{XC}(\vec{r}, \vec{r}')$ in Eq. (15) is the product of a density prefactor $n(\vec{r}')$ and the integrated pair correlation function g. Because of the limited knowledge about g for inhomogeneous systems, it is natural to start by using the pair correlation function of the homogeneous electron liquid $g_n^h(r;\lambda)$, where r is the relative distance between the electrons in the considered pair. Then it remains to make a choice of an approximate density prefactor and a suitable density argument n.

In the LD approximation (16) the prefactor $n(\vec{r}')$ is replaced by $n(\vec{r})$ for all values of $\vec{r}'$. This is obviously a good approximation only for $\vec{r} \simeq \vec{r}'$, a region which is unimportant in Eq. (1), due to the volume element d^3r'. If the prefactor should be approximated, the replacement should assure that $n_{XC}(\vec{r}, \vec{r}')$ is described as well as possible over the major range of the XC hole, i.e., for $|\vec{r} - \vec{r}'| \lesssim k_F^{-1}(n(\vec{r}))$. A suitable average of the density, $n(\vec{r})$, could be such a prefactor approximation. In addition, due to the nonzero range of the XC forces, $\epsilon_{XC}(\vec{r})$ [Eq. (19)] should not only depend on the density in the point $\vec{r}$, as it does in the LD approximation, but on the density in all points within a distance of the order of $k_F^{-1}(n(\vec{r}))$ from $\vec{r}$.

These features can be incorporated by assuming the following form of the XC hole:

$$n_{XC}(\vec{r}, \vec{r}') \simeq \bar{n}(\vec{r}) \int_0^1 [g^h_{\bar{n}(\vec{r})}(\vec{r} - \vec{r}'; \lambda) - 1] \, d\lambda , \tag{20}$$

with

$$\bar{n}(\vec{r}) = \int w(\vec{r} - \vec{r}', \bar{n}(\vec{r})) n(\vec{r}') \, d^3r' , \tag{21}$$

where w is a weight function to be determined below.

In this *average-density* (AD) *approximation*[16] the XC energy functional becomes

$$E_{XC}\{n\} \simeq \int n(\vec{r}) \epsilon_{XC}(\bar{n}(\vec{r})) \, d^3r . \tag{22}$$

The functional satisfies both criteria (a) and (b) above; the latter is fulfilled because the pair correlation function of the homogeneous medium automatically gives a hole containing one unit charge. Below, we will choose $w(\vec{r} - \vec{r}', \bar{n}(\vec{r}))$, so that it is large for $|\vec{r} - \vec{r}'| \lesssim k_F(\bar{n}(\vec{r}))^{-1}$, implying that the density is sampled over a physically reasonable region. Finally, the use of $\bar{n}(\vec{r})$ instead of a $n(\vec{r})$ in front of the bracket in Eq. (20) means that the region, where the exact and approximate $n_{XC}^{SA}(\vec{r}, r'')$ are close to each other, tends to be displaced from the point $|\vec{r}| = r''$. Because the sizes of the hole and the weight function w are of the same order of magnitude, this displacement has a physical size.

The weight function w could be chosen in several ways. The one that we propose is constructed by making maximal use of the present knowledge of the weakly inhomogeneous electron liquid. In particular, we require that in the limit of weak variations in the density, i.e., for $|\Delta n/n_0| \ll 1$, our functional should reduce to the expression (3), which *in this limit* is exact. Together with some physically motivated additional conditions, this requirement uniquely determines $w(r', \bar{n}(\vec{r}))$, as is discussed in Appendix C. To calculate w, we apply Eqs. (20) and (21) to a system with the density given by Eqs. (10) and (11). Requiring that the weight function is normalized,

$$\int w(\vec{r}', \bar{n}(\vec{r}))\, d^3r' = 1\,, \tag{23}$$

Equation (21) can be written

$$\bar{n}(\vec{r}) = n_0 + \int w(\vec{r} - \vec{r}', n(\vec{r}))\Delta n(\vec{r}')\, d^3r'$$

$$\equiv n_0 + \Delta\bar{n}(\vec{r})\,. \tag{24}$$

Expanding Eq. (20) to second order in $\Delta n(\vec{r})$ gives

$$E_{\rm XC}\{n\} = \int d^3r\, n_0 \epsilon_{\rm XC}(n_0) + \int d^3r\, n_0 \frac{\partial \epsilon_{\rm XC}}{\partial n}\Delta\bar{n}(\vec{r}) + \int d^3r \left(\frac{\partial \epsilon_{\rm XC}}{\partial n}\Delta n(\vec{r})\Delta\bar{n}(\vec{r}) + \frac{1}{2} n_0 \frac{\partial^2 \epsilon_{\rm XC}}{\partial n^2}[\Delta\bar{n}(\vec{r})]^2 \right), \tag{25}$$

where the derivatives are taken at the density n_0. Using Eqs. (11) and (23), we find to second order in $\Delta n(\vec{r})$

$$\int d^3r\, \Delta\bar{n}(\vec{r}) = \int d^3r \int d^3r' \int d^3r'' \frac{\partial w}{\partial n}(\vec{r} - \vec{r}', n_0) w(\vec{r} - \vec{r}'', n_0)\Delta n(\vec{r}')\Delta n(\vec{r}'')\,. \tag{26}$$

Identifying with Eq. (3) gives

$$\tfrac{1}{2} K_{\rm XC}(\vec{r} - \vec{r}', n_0) = n_0 \frac{\partial \epsilon_{\rm XC}}{\partial n} \int d^3r'' \frac{\partial w}{\partial n}(\vec{r}'' - \vec{r}, n_0) w(\vec{r}'' - \vec{r}', n_0) + \frac{\partial \epsilon_{\rm XC}}{\partial n}(n_0) w(\vec{r} - \vec{r}', n_0) + \frac{1}{2} n_0 \frac{\partial^2 \epsilon_{\rm XC}}{\partial n}(n_0) \int d^3r'' w(\vec{r}'' - \vec{r}, n_0) w(\vec{r}'' - \vec{r}', n_0)\,. \tag{27}$$

Requiring $w(\vec{r}) = w(-\vec{r})$, we get after Fourier transformation

$$\tfrac{1}{2} K_{\rm XC}(k, n_0) = n_0 \frac{\partial \epsilon_{\rm xc}(n_0)}{\partial n} w(k, n_0) \frac{\partial w(k, n_0)}{\partial n} + \frac{\partial \epsilon_{\rm xc}(n_0)}{\partial n} w(k, n_0) + \tfrac{1}{2} n_0 \frac{\partial^2 \epsilon_{\rm xc}(n_0)}{\partial n^2}[w(k, n_0)]^2\,. \tag{28}$$

This equation relates w to parameters of the homogeneous electron liquid, as $K_{\rm XC}$ can be directly expressed in the dielectric function $\epsilon(k)$ of that system,[2]

$$K_{\rm XC}(k, n_0) = (4\pi e^2/k^2)\{[\epsilon(k, n_0) - 1]^{-1} - [\epsilon_{\rm RPA}(k, n_0) - 1]^{-1}\}, \tag{29}$$

where $\epsilon_{\rm RPA}(k, n)$ is the dielectric function of the homogeneous electron gas in the random-phase approximation.

We rewrite Eq. (28) as

$$[w(k, r_s)]^2 + 2A(r_s) w(k, r_s)\left(1 - \frac{1}{3} r_s \frac{\partial w(k, r_s)}{\partial r_s}\right) - [1 + 2A(r_s)]\, f(k, r_s) = 0\,, \tag{30}$$

where

$$f(k, r_s) = K_{\rm XC}(k, r_s)/K_{\rm XC}(0, r_s)\,,$$

$$A(r_s) = \left.\frac{\partial \epsilon_{\rm XC}(n)/\partial n}{n\partial^2 \epsilon_{\rm XC}(n)/\partial n^2}\right|_{n=n_0}$$

and

$$\tfrac{4}{3}\pi r_s^3 = 1/n_0\,.$$

We have used the relation

$$K_{\rm xc}(0, n) = 2\frac{\partial \epsilon_{\rm XC}}{\partial n} + n\frac{\partial^2 \epsilon_{\rm XC}(n)}{\partial n^2}, \tag{31}$$

which follows from the compressibility sum rule.

The properties and the solution of Eq. (30) are discussed in Appendix C. To represent the solution, it is convenient to use the dimensionless variable $q = k/k_F(r_s)$, as

$$\tilde{w}(q, r_s) = w(qk_F(r_s), r_s) \tag{32}$$

for given q has a smooth dependence on r_s. We present data for $\tilde{w}(q, r_s)$ in Fig. 9 and Table I. The weight function $\tilde{w}(q, r_s)$ has a range ~2, which can be traced to the range ~$2k_F$ of $K_{\rm XC}(k, r_s)$. As should be expected for physical reasons, this

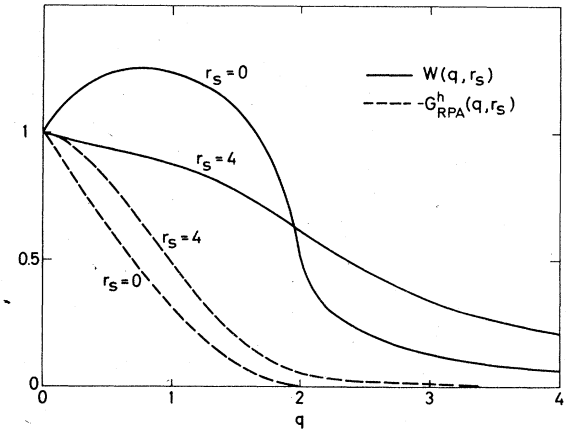

FIG. 9. Fourier transform of the sampling function $w(\vec{r} - \vec{r}'; \bar{n}(r'))$ [Eq. (21)] (full curves) and the correlation function $G^h_{\rm RPA}(q, \bar{n})$ [Eq. (38)] (dashed curve), ($q = k/k_F$).

TABLE I. Solution $w(q, r_s)$ of the differential equation (28) tabulated as a function of $q=k/k_F$ and r_s.

q \ r_s	0.0	0.5	1.0	1.5	2.0	2.5	3.0	3.5	4.0	4.5	5.0	5.5	6.0
0.0	1.000	1.000	1.000	1.000	1.000	1.000	1.000	1.000	1.000	1.000	1.000	1.000	1.000
0.05	1.044	0.993	0.991	0.991	0.991	0.990	0.990	0.990	0.990	0.991	0.991	0.991	0.992
0.10	1.081	0.989	0.985	0.984	0.983	0.983	0.983	0.983	0.982	0.982	0.982	0.982	0.982
0.15	1.112	0.986	0.981	0.979	0.977	0.977	0.976	0.976	0.975	0.975	0.975	0.975	0.975
0.20	1.138	0.982	0.977	0.974	0.972	0.970	0.970	0.969	0.969	0.968	0.968	0.968	0.968
0.25	1.160	0.980	0.973	0.969	0.966	0.965	0.964	0.963	0.962	0.962	0.962	0.961	0.961
0.30	1.179	0.978	0.969	0.966	0.962	0.959	0.958	0.957	0.956	0.955	0.955	0.955	0.954
0.35	1.195	0.976	0.964	0.962	0.958	0.954	0.952	0.951	0.950	0.949	0.949	0.948	0.948
0.40	1.208	0.974	0.959	0.957	0.954	0.950	0.947	0.945	0.944	0.943	0.943	0.942	0.941
0.45	1.220	0.973	0.955	0.953	0.950	0.946	0.942	0.940	0.939	0.937	0.936	0.936	0.935
0.50	1.230	0.972	0.950	0.947	0.945	0.941	0.938	0.935	0.933	0.932	0.930	0.930	0.929
0.55	1.237	0.970	0.945	0.942	0.940	0.937	0.933	0.930	0.928	0.926	0.924	0.923	0.923
0.60	1.244	0.968	0.941	0.937	0.934	0.932	0.929	0.925	0.922	0.920	0.919	0.917	0.916
0.65	1.248	0.965	0.936	0.931	0.928	0.927	0.924	0.920	0.917	0.915	0.913	0.911	0.910
0.70	1.251	0.964	0.930	0.925	0.922	0.921	0.919	0.916	0.912	0.909	0.907	0.906	0.904
0.75	1.253	0.964	0.925	0.920	0.916	0.915	0.913	0.911	0.907	0.904	0.902	0.900	0.898
0.80	1.253	0.964	0.919	0.913	0.909	0.908	0.907	0.906	0.902	0.899	0.896	0.894	0.892
0.85	1.252	0.964	0.913	0.907	0.902	0.901	0.901	0.900	0.897	0.894	0.891	0.888	0.886
0.90	1.250	0.964	0.906	0.900	0.895	0.893	0.893	0.893	0.892	0.888	0.885	0.882	0.880
0.95	1.246	0.963	0.899	0.893	0.888	0.886	0.886	0.886	0.885	0.883	0.880	0.877	0.874
1.00	1.241	0.962	0.891	0.886	0.880	0.878	0.878	0.879	0.879	0.877	0.874	0.871	0.868
1.05	1.235	0.959	0.882	0.878	0.872	0.870	0.870	0.871	0.872	0.871	0.869	0.865	0.862
1.10	1.227	0.956	0.872	0.870	0.863	0.861	0.861	0.863	0.864	0.864	0.862	0.859	0.856
1.15	1.218	0.952	0.861	0.861	0.854	0.852	0.852	0.854	0.856	0.856	0.856	0.853	0.850
1.20	1.207	0.946	0.849	0.851	0.844	0.842	0.843	0.844	0.847	0.848	0.848	0.847	0.844
1.25	1.194	0.940	0.836	0.841	0.834	0.832	0.833	0.835	0.837	0.840	0.840	0.840	0.838
1.30	1.179	0.932	0.821	0.830	0.823	0.822	0.822	0.824	0.827	0.830	0.832	0.832	0.831
1.35	1.163	0.923	0.807	0.818	0.811	0.810	0.811	0.814	0.817	0.820	0.823	0.824	0.824
1.40	1.144	0.911	0.794	0.805	0.799	0.798	0.799	0.802	0.806	0.810	0.813	0.815	0.816
1.45	1.123	0.897	0.780	0.791	0.786	0.786	0.787	0.790	0.794	0.799	0.803	0.806	0.807
1.50	1.099	0.882	0.765	0.776	0.771	0.772	0.774	0.777	0.782	0.787	0.792	0.796	0.798
1.55	1.072	0.865	0.749	0.760	0.756	0.757	0.760	0.764	0.769	0.775	0.780	0.785	0.788
1.60	1.041	0.843	0.732	0.742	0.739	0.742	0.745	0.750	0.755	0.762	0.768	0.773	0.777
1.65	1.005	0.819	0.713	0.723	0.721	0.725	0.729	0.735	0.741	0.748	0.754	0.761	0.766
1.70	0.965	0.793	0.692	0.702	0.702	0.707	0.712	0.719	0.725	0.733	0.740	0.747	0.753
1.75	0.918	0.763	0.669	0.679	0.682	0.688	0.694	0.701	0.709	0.717	0.725	0.733	0.740
1.80	0.863	0.722	0.643	0.653	0.659	0.667	0.675	0.683	0.691	0.700	0.709	0.718	0.726
1.85	0.798	0.682	0.616	0.626	0.635	0.645	0.654	0.664	0.673	0.683	0.692	0.702	0.711
1.90	0.719	0.632	0.585	0.597	0.610	0.621	0.632	0.643	0.653	0.664	0.675	0.685	0.695
1.95	0.620	0.574	0.552	0.565	0.582	0.596	0.609	0.621	0.633	0.644	0.656	0.667	0.678
2.00	0.507	0.523	0.519	0.535	0.555	0.571	0.586	0.599	0.612	0.624	0.637	0.649	0.660
2.05	0.428	0.464	0.490	0.510	0.531	0.548	0.564	0.579	0.592	0.606	0.618	0.631	0.644
2.10	0.378	0.432	0.464	0.487	0.510	0.528	0.545	0.561	0.575	0.588	0.602	0.615	0.628
2.15	0.342	0.399	0.441	0.467	0.490	0.510	0.527	0.543	0.558	0.572	0.585	0.599	0.612
2.20	0.317	0.378	0.421	0.447	0.471	0.492	0.510	0.527	0.542	0.556	0.570	0.584	0.597
2.25	0.291	0.355	0.401	0.429	0.454	0.475	0.494	0.511	0.526	0.541	0.555	0.569	0.583
2.30	0.269	0.336	0.384	0.412	0.438	0.460	0.479	0.496	0.512	0.526	0.541	0.555	0.568
2.35	0.250	0.318	0.367	0.396	0.423	0.445	0.464	0.482	0.498	0.512	0.527	0.541	0.555
2.40	0.232	0.302	0.352	0.381	0.408	0.430	0.450	0.468	0.484	0.499	0.513	0.527	0.541
2.45	0.217	0.287	0.337	0.367	0.394	0.417	0.437	0.455	0.471	0.486	0.500	0.514	0.528
2.50	0.203	0.274	0.324	0.354	0.381	0.404	0.424	0.442	0.458	0.473	0.487	0.502	0.516
2.55	0.192	0.261	0.311	0.342	0.369	0.392	0.412	0.430	0.446	0.461	0.475	0.489	0.504
2.60	0.183	0.250	0.299	0.330	0.357	0.380	0.400	0.418	0.434	0.449	0.463	0.478	0.492
2.65	0.175	0.240	0.288	0.319	0.346	0.368	0.389	0.407	0.423	0.438	0.452	0.466	0.480
2.70	0.167	0.231	0.278	0.308	0.336	0.358	0.378	0.396	0.412	0.427	0.441	0.455	0.469
2.75	0.159	0.221	0.268	0.298	0.325	0.347	0.367	0.385	0.401	0.416	0.430	0.444	0.458
2.80	0.152	0.213	0.258	0.288	0.315	0.337	0.357	0.375	0.391	0.406	0.420	0.433	0.447
2.85	0.145	0.205	0.249	0.279	0.305	0.327	0.347	0.365	0.381	0.396	0.410	0.423	0.437
2.90	0.139	0.197	0.241	0.270	0.296	0.318	0.338	0.356	0.371	0.386	0.400	0.413	0.427
2.95	0.133	0.190	0.233	0.262	0.287	0.309	0.329	0.346	0.362	0.377	0.390	0.403	0.417

TABLE I. (*Continued*)

q \ r_s	0.0	0.5	1.0	1.5	2.0	2.5	3.0	3.5	4.0	4.5	5.0	5.5	6.0
3.00	0.127	0.183	0.225	0.254	0.279	0.300	0.320	0.337	0.353	0.367	0.381	0.394	0.407
3.05	0.124	0.177	0.218	0.246	0.271	0.292	0.311	0.329	0.344	0.358	0.372	0.385	0.398
3.10	0.120	0.171	0.211	0.239	0.263	0.284	0.303	0.320	0.336	0.350	0.363	0.376	0.389
3.15	0.116	0.161	0.204	0.231	0.256	0.276	0.295	0.312	0.328	0.341	0.355	0.367	0.380
3.20	0.111	0.160	0.198	0.224	0.248	0.269	0.288	0.304	0.320	0.333	0.346	0.359	0.371
3.25	0.107	0.154	0.192	0.218	0.242	0.262	0.280	0.297	0.312	0.325	0.338	0.351	0.363
3.30	0.102	0.150	0.186	0.212	0.235	0.255	0.273	0.290	0.304	0.318	0.330	0.343	0.355
3.35	0.098	0.145	0.181	0.206	0.229	0.248	0.266	0.282	0.297	0.310	0.323	0.335	0.347
3.40	0.094	0.139	0.175	0.200	0.223	0.242	0.260	0.275	0.290	0.303	0.315	0.327	0.339
3.45	0.090	0.135	0.170	0.195	0.217	0.236	0.253	0.269	0.283	0.296	0.308	0.320	0.331
3.50	0.086	0.131	0.166	0.189	0.211	0.230	0.247	0.262	0.276	0.289	0.301	0.312	0.324
3.55	0.082	0.127	0.161	0.184	0.205	0.224	0.241	0.256	0.270	0.282	0.294	0.305	0.316
3.60	0.077	0.123	0.157	0.179	0.200	0.218	0.235	0.250	0.263	0.276	0.287	0.298	0.309
3.65	0.074	0.119	0.152	0.175	0.195	0.213	0.229	0.244	0.257	0.269	0.281	0.291	0.302
3.70	0.071	0.115	0.148	0.170	0.190	0.208	0.224	0.238	0.251	0.263	0.274	0.285	0.295
3.75	0.068	0.112	0.143	0.165	0.185	0.203	0.218	0.232	0.245	0.257	0.268	0.278	0.289
3.80	0.066	0.109	0.139	0.161	0.180	0.198	0.213	0.226	0.239	0.251	0.261	0.272	0.282
3.85	0.063	0.106	0.135	0.157	0.176	0.193	0.208	0.221	0.233	0.245	0.255	0.265	0.275
3.90	0.061	0.102	0.132	0.153	0.172	0.188	0.203	0.216	0.228	0.239	0.249	0.259	0.269
3.95	0.060	0.099	0.128	0.149	0.167	0.184	0.198	0.210	0.222	0.233	0.243	0.253	0.262

range is thus of the same order as the inverse size of the exchange-correlation hole.

Of interest is also the case when only exchange effects are included. As discussed in Appendix C, Eq. (30) then has an r_s-independent solution $\tilde{w}_{ex}(q)$. This solution is identical with the solution for $r_s = 0$ that includes both exchange and correlation effects. This simply reflects that effects due to correlation are negligible compared to those of exchange for $r_s = 0$.

According to Eqs. (9) and (22) the XC potential in the AD approximation is

$$v_{XC}^{AD}(\vec{r}) = \epsilon_{XC}(\bar{n}(\vec{r})) + \int d^3r' n(\vec{r}') \frac{d\epsilon_{xc}}{dn}\bigg|_{n=\bar{n}(\vec{r}')} \times \frac{\delta\bar{n}(\vec{r}')}{\delta n(\vec{r})}, \tag{33}$$

where the functional derivative can be evaluated from Eq. (21),

$$\frac{\delta\bar{n}(\vec{r}')}{\delta n(\vec{r})} = w(\vec{r} - \vec{r}', \bar{n}(\vec{r})) \times \left(1 - \int d^3r'' n(\vec{r}'') \frac{\partial w(\vec{r}' - \vec{r}'', n)}{\partial n}\bigg|_{n=\bar{n}(\vec{r}')}\right)^{-1}. \tag{34}$$

C. Weighted-density approximation

The fundamental features built into the AD approximation, i.e., the charge-conservation sum rule (18) and the dependence of the XC energy density $\epsilon_{XC}(\vec{r})$ not only on the density at $\vec{r}$ but on the density at all points within a certain range from $\vec{r}$, can be included also in other schemes.

We shall here describe one such scheme, which we have called the *weighted-density* (WD) *approximation*.[17,18] Like in the AD scheme, the exact pair correlation function is replaced with that of a homogeneous electron gas. The essential difference is that we keep *the proper density prefactor* $n(r')$ in expression (15) for the XC charge density, i.e.,

$$n_{XC}^{WD}(\vec{r}, \vec{r}') = n(\vec{r}') \int_0^1 d\lambda [g^h_{\tilde{n}(\vec{r})}(\vec{r} - \vec{r}'; \lambda) - 1]. \tag{35}$$

The density argument $\tilde{n}(\vec{r})$ in Eq. (35) is determined from the sum rule (18):

$$\int d^3r' \int_0^1 d\lambda [g^h_{\tilde{n}(r)}(\vec{r} - \vec{r}'; \lambda) - 1] n(\vec{r}') = -1. \tag{36}$$

In the WD approximation then, for each point $\vec{r}$ we determine an $\tilde{n}(\vec{r})$ that satisfies the sum rule (36). This is then used in Eqs. (35) and (14) to calculate the XC energy E_{XC}.

The major qualitative difference between the AD and WD approximations is that due to the prefactor $n(\vec{r}')$ of Eq. (35) the XC hole $n_{XC}^{WD}(\vec{r}, \vec{r}')$ may be asymmetric with respect to $\vec{r}$. In practice, however, this apparent improvement compared with the spherical AD hole has no influence on E_{xc}. Equation (19) shows that only the spherical average of the XC hole enters the expression for the XC energy. Another difference concerns the limit of

weak density variations, where the AD approximation, unlike the WD one, is exact. As both approximation schemes reduce to the exact form when the density is *precisely* constant, however, only numerical tests can tell whether for real systems this difference is significant.

The WD scheme requires as input the pair correlation function $g^h(r)$ of a homogeneous electron gas, or equivalently its Fourier transform, the static structure factor $S(q)$. It is convenient to introduce a correlation function $G^h(\vec{r}-\vec{r}';n)$, defined by Eqs. (15) and (35), with the Fourier transform

$$G^h(q;n)=\frac{1}{n}\int_0^1 d\lambda\,[1-S(q,\lambda;n)]\,. \tag{37}$$

Although $S(q)$ is not known exactly, several approximate schemes of varying sophistication are available in the literature.[19] For illustrational purpose we shall here content ourselves with the simplest one that includes correlation effects, the random-phase approximation (RPA). Here the integration over the coupling constant λ in Eq. (36) can be performed analytically

$$G^h_{\mathrm{RPA}}(q,n)=\frac{1}{n}\left(\frac{1}{n}\int_0^\infty\frac{d\omega}{\pi}\frac{1}{v(q)}\ln[1-v(q)\chi^0(q,i\omega)]+1\right)_{n=\tilde{n}}, \tag{38}$$

where χ^0 is the Lindhard density response function and $v(q)=4\pi e^2/q^2$. In Table II G^h_{RPA} is tabulated as a function of $q\equiv k/k_F$ and n. The comparison with $w(q)$ in Fig. 9 shows that $G(q)$ decays much faster than $w(q)$. This means that in real space $w(r,\bar{n})$ samples a smaller volume than $\tilde{n}G(r,\tilde{n})$–provided that $\tilde{n}$ and $\bar{n}$ are comparable.

The implications of this and the previously mentioned differences between the two schemes have to be tested by numerical calculations for real systems. This is the scope of the following sections.

According to Eqs. (14), (15), and (35) the XC energy density of the WD approximation is

$$\epsilon^{\mathrm{WD}}_{\mathrm{XC}}(\vec{r})=\frac{1}{2}\int d^3r'v(\vec{r}-\vec{r}')n(\vec{r}')G^h(\vec{r}-\vec{r}';\tilde{n}(\vec{r}))\,, \tag{39}$$

where $v(r)=e^2/r$. The functional derivative (9) gives the following expression for the corresponding XC potential:

$$\begin{aligned}v^{\mathrm{WD}}_{\mathrm{XC}}(\vec{r})&=\epsilon^{\mathrm{WD}}_{\mathrm{XC}}(\vec{r})+\frac{1}{2}\int d^3r'v(\vec{r}-\vec{r}')n(\vec{r}')G^h(\vec{r}-\vec{r}';\tilde{n}(\vec{r}'))\\&+\frac{1}{2}\int d^3r''n(\vec{r}'')\int d^3r'v(\vec{r}''-\vec{r}')n(\vec{r}')\frac{\partial G^h(\vec{r}''-\vec{r}';n)}{\partial n}\bigg|_{n=\tilde{n}(\vec{r}')}\frac{\delta\tilde{n}(\vec{r}')}{\delta n(\vec{r})}\,,\end{aligned} \tag{40}$$

where the functional derivative can be evaluated from Eq. (36):

$$\frac{\delta\bar{n}(\vec{r}')}{\delta n(\vec{r})}=-G^h(\vec{r}'-\vec{r};\tilde{n}(\vec{r}'))\Big/\int d^3r''n(\vec{r}'')\frac{\partial G^h(\vec{r}'-\vec{r}'';n)}{\partial n}\bigg|_{n=\tilde{n}(\vec{r}')}. \tag{41}$$

Thus $v^{\mathrm{WD}}_{\mathrm{XC}}$ may be expressed entirely in G^h and $\partial G^h/\partial n$.

D. Shell partitioning

As will be illustrated in Secs. IV and V the AD and WD approximations give good accounts for the XC properties of different systems. Being approximate, however, it is certainly worthwhile to explore the possibility of further improved procedures of comparable simplicity. Here we will propose one such procedure which improves the modeling of intershell correlations.

The above approach to the description of inhomogeneous electron systems is based on a philosophy that views the inhomogeneous system as formed by a gradual deformation of an originally homogeneous electron liquid. The deformation is supposed not to alter the qualitative XC characteristics of the electrons. To be more specific, the replacement of the true pair correlation function g in Eq. (15) by the one for the homogeneous liquid g^h in the AD and WD approximations involves basically two assumptions: (a) The only forces that keep electrons apart are due to exchange and correlation, and (b) the effects of these forces are the same as in the homogeneous electron liquid with the appropriate density. Other mechanisms that keep electrons apart, e.g., external potentials that in an essential way break the continuous translational symmetry of the homogeneous liquid and localize the electrons to certain regions, cannot formally be modeled in this manner.

An important example of such a mechanism is the electron-shell formation in atoms, molecules, and solids, which is due to the dominance of the spherical nuclear potential close to the nuclei. The electrons within a particular shell are energetically and spatially distinguished from those of another shell, so distinctly that they may be thought

TABLE II. Function $G^h_{\mathrm{RPA}}(q, r_s)$ [Eq. (38)] as a function of $q = k/k_F$ and r_s ($\frac{4}{3}\pi r_s^3 = 1/n$).

q \ r_s	0.0	0.2	0.4	0.6	0.8	1.0	1.5	2.0	2.5	3.0	3.5	4.0	4.5	5.0	5.5	6.0
0.0	−1.000	−1.000	−1.000	−1.000	−1.000	−1.000	−1.000	−1.000	−1.000	−1.000	−1.000	−1.000	−1.000	−1.000	−1.000	−1.000
0.050	−0.964	−0.990	−0.993	−0.994	−0.995	−0.995	−0.996	−0.997	−0.997	−0.997	−0.997	−0.998	−0.998	−0.998	−0.998	−0.998
0.100	−0.926	−0.966	−0.973	−0.977	−0.980	−0.982	−0.985	−0.987	−0.988	−0.989	−0.990	−0.990	−0.991	−0.991	−0.992	−0.992
0.150	−0.888	−0.933	−0.946	−0.953	−0.958	−0.962	−0.967	−0.971	−0.974	−0.976	−0.977	−0.979	−0.980	−0.981	−0.982	−0.982
0.200	−0.851	−0.897	−0.914	−0.924	−0.931	−0.937	−0.945	−0.951	−0.955	−0.959	−0.961	−0.963	−0.965	−0.967	−0.968	−0.969
0.250	−0.814	−0.859	−0.879	−0.892	−0.901	−0.907	−0.920	−0.928	−0.933	−0.938	−0.942	−0.945	−0.947	−0.950	−0.952	−0.953
0.300	−0.777	−0.819	−0.842	−0.856	−0.867	−0.876	−0.891	−0.901	−0.908	−0.914	−0.919	−0.923	−0.927	−0.930	−0.933	−0.935
0.350	−0.740	−0.780	−0.803	−0.820	−0.832	−0.841	−0.859	−0.872	−0.881	−0.888	−0.894	−0.900	−0.904	−0.908	−0.911	−0.914
0.400	−0.704	−0.741	−0.765	−0.782	−0.795	−0.806	−0.826	−0.840	−0.851	−0.860	−0.867	−0.873	−0.879	−0.883	−0.887	−0.891
0.450	−0.668	−0.703	−0.726	−0.744	−0.758	−0.769	−0.791	−0.808	−0.820	−0.830	−0.838	−0.846	−0.852	−0.857	−0.862	−0.866
0.500	−0.633	−0.665	−0.688	−0.706	−0.720	−0.732	−0.756	−0.774	−0.787	−0.799	−0.808	−0.816	−0.823	−0.829	−0.835	−0.840
0.550	−0.598	−0.628	−0.650	−0.668	−0.682	−0.695	−0.720	−0.739	−0.754	−0.766	−0.776	−0.785	−0.793	−0.800	−0.807	−0.812
0.600	−0.564	−0.591	−0.613	−0.630	−0.645	−0.658	−0.683	−0.703	−0.719	−0.733	−0.744	−0.754	−0.762	−0.770	−0.777	−0.783
0.650	−0.530	−0.555	−0.576	−0.593	−0.608	−0.621	−0.647	−0.668	−0.684	−0.699	−0.711	−0.721	−0.731	−0.739	−0.746	−0.753
0.700	−0.497	−0.520	−0.540	−0.557	−0.571	−0.584	−0.611	−0.632	−0.649	−0.664	−0.677	−0.688	−0.698	−0.707	−0.715	−0.722
0.750	−0.464	−0.486	−0.505	−0.521	−0.535	−0.548	−0.575	−0.596	−0.614	−0.630	−0.643	−0.655	−0.665	−0.675	−0.683	−0.691
0.800	−0.432	−0.453	−0.470	−0.486	−0.500	−0.512	−0.539	−0.561	−0.579	−0.595	−0.609	−0.621	−0.632	−0.642	−0.651	−0.659
0.850	−0.401	−0.420	−0.437	−0.452	−0.465	−0.478	−0.504	−0.526	−0.544	−0.560	−0.575	−0.587	−0.599	−0.609	−0.619	−0.627
0.900	−0.371	−0.389	−0.404	−0.419	−0.432	−0.444	−0.469	−0.491	−0.510	−0.526	−0.541	−0.554	−0.565	−0.576	−0.586	−0.595
0.950	−0.341	−0.358	−0.373	−0.386	−0.399	−0.410	−0.436	−0.457	−0.476	−0.492	−0.507	−0.520	−0.532	−0.543	−0.553	−0.563
1.000	−0.313	−0.328	−0.342	−0.355	−0.367	−0.378	−0.403	−0.424	−0.443	−0.459	−0.474	−0.487	−0.500	−0.511	−0.521	−0.531
1.050	−0.285	−0.299	−0.313	−0.325	−0.337	−0.347	−0.371	−0.392	−0.410	−0.427	−0.442	−0.455	−0.467	−0.479	−0.489	−0.499
1.100	−0.258	−0.272	−0.284	−0.296	−0.807	−0.317	−0.340	−0.361	−0.379	−0.395	−0.410	−0.423	−0.435	−0.447	−0.457	−0.467
1.150	−0.233	−0.245	−0.257	−0.268	−0.279	−0.288	−0.311	−0.330	−0.348	−0.364	−0.379	−0.392	−0.404	−0.416	−0.426	−0.436
1.200	−0.208	−0.220	−0.231	−0.241	−0.251	−0.261	−0.282	−0.301	−0.318	−0.334	−0.348	−0.362	−0.374	−0.385	−0.396	−0.406
1.250	−0.185	−0.196	−0.206	−0.216	−0.225	−0.234	−0.255	−0.273	−0.290	−0.305	−0.319	−0.332	−0.344	−0.356	−0.366	−0.376
1.300	−0.162	−0.173	−0.182	−0.192	−0.201	−0.209	−0.229	−0.246	−0.263	−0.277	−0.291	−0.304	−0.316	−0.327	−0.338	−0.347
1.350	−0.141	−0.151	−0.160	−0.169	−0.177	−0.185	−0.204	−0.221	−0.236	−0.251	−0.264	−0.277	−0.288	−0.299	−0.310	−0.320
1.400	−0.122	−0.130	−0.139	−0.147	−0.155	−0.163	−0.180	−0.197	−0.212	−0.226	−0.239	−0.251	−0.262	−0.273	−0.283	−0.293
1.450	−0.103	−0.111	−0.119	−0.127	−0.134	−0.142	−0.158	−0.174	−0.188	−0.202	−0.214	−0.226	−0.237	−0.247	−0.257	−0.267
1.500	−0.086	−0.094	−0.101	−0.108	−0.115	−0.122	−0.138	−0.152	−0.166	−0.179	−0.191	−0.202	−0.213	−0.223	−0.233	−0.242
1.550	−0.070	−0.077	−0.084	−0.091	−0.097	−0.104	−0.119	−0.133	−0.146	−0.158	−0.169	−0.180	−0.191	−0.201	−0.210	−0.219
1.600	−0.056	−0.063	−0.069	−0.075	−0.081	−0.087	−0.101	−0.114	−0.127	−0.138	−0.149	−0.160	−0.170	−0.179	−0.188	−0.197
1.650	−0.043	−0.049	−0.055	−0.061	−0.067	−0.072	−0.085	−0.098	−0.109	−0.120	−0.131	−0.141	−0.150	−0.159	−0.168	−0.176
1.700	−0.032	−0.038	−0.043	−0.048	−0.054	−0.059	−0.071	−0.082	−0.093	−0.104	−0.114	−0.123	−0.132	−0.141	−0.149	−0.157
1.750	−0.023	−0.028	−0.033	−0.038	−0.042	−0.047	−0.058	−0.069	−0.079	−0.089	−0.098	−0.107	−0.116	−0.124	−0.132	−0.140
1.800	−0.015	−0.019	−0.024	−0.028	−0.033	−0.037	−0.048	−0.057	−0.067	−0.076	−0.085	−0.093	−0.102	−0.109	−0.117	−0.124
1.850	−0.008	−0.013	−0.017	−0.021	−0.025	−0.029	−0.038	−0.048	−0.057	−0.065	−0.073	−0.081	−0.089	−0.096	−0.103	−0.110
1.900	−0.004	−0.008	−0.011	−0.015	−0.019	−0.022	−0.031	−0.040	−0.048	−0.056	−0.063	−0.071	−0.078	−0.085	−0.092	−0.098
1.950	−0.001	−0.004	−0.008	−0.011	−0.015	−0.018	−0.026	−0.034	−0.041	−0.048	−0.055	−0.062	−0.069	−0.075	−0.082	−0.088
2.000	−0.000	−0.003	−0.006	−0.009	−0.012	−0.015	−0.023	−0.030	−0.037	−0.043	−0.050	−0.056	−0.062	−0.068	−0.074	−0.079

of as forming a one-liquid system. The *intrashell* XC effects should therefore be covered by the above philosophy. The *intershell* correlations, on the other hand, should not, as they involve at least two different liquids.

These aspects are relevant also for the LD approximation,[20] but they are emphasized by the density-sampling procedure in the AD and WD schemes. The problems are most clearly spelled out in the regions with very strong density variations between the electron shells. For instance, the very high density in the core region would have a substantial influence on the XC energy density in the valence region via the integrations over $w(\vec{r}-\vec{r}';\bar{n}(\vec{r}))$ in Eq. (21) and over $g^h(\vec{r}-\vec{r}';\lambda,\tilde{n}(\vec{r}))$ in Eq. (36). The result would be that $\bar{n}(\vec{r})$ and $\tilde{n}(\vec{r})$ would be exaggerated in the valence region, and the intershell contribution to the XC energy would be overestimated. More explicit arguments may be given if only exchange effects are available: It is illuminating to consider the following exact expression for the exchange-energy density (here given for a spin-compensated system)

$$\epsilon_x(\vec{r}) = \frac{e^2}{2}\int \frac{n_x(\vec{r},\vec{r}')}{|\vec{r}-\vec{r}'|}\,d^3r' = -2e^2\sum_{ij}\frac{\Psi_{i\sigma}(\vec{r})\Psi_{j\sigma}(\vec{r})}{n(\vec{r})}\int d^3r'\frac{\Psi_{i\sigma}(\vec{r}')\Psi_{j\sigma}(\vec{r}')}{|\vec{r}-\vec{r}'|}. \tag{42}$$

As is clear from Eq. (42) *both* $\Psi_{i\sigma}(\vec{r})$ *and* $\Psi_{j\sigma}(\vec{r})$ have to be nonzero in order to give a finite contribution to $\epsilon_x(\vec{r})$. It follows that intershell contributions, i.e., when, say, $\Psi_{i\sigma}$ is a core orbital and $\Psi_{j\sigma}$ is a valence orbital, vanish outside the core region, while the AD and WD approximations give a nonzero contribution. On the other hand, the LD approximation correctly leads to zero intershell exchange-energy density outside the core region as it only uses the local density. Rather than using the total density, the above arguments suggest that the averaging should be performed only within each shell and that a LD-type approximation should be used for the intershell effects.

In the average-density shell-partitioned (ADS) scheme the average density of shell i at point $\vec{r}$ is defined by

$$\bar{n}_i(\vec{r}) = \sum_{j\neq i} n_j(\vec{r}) + \int d^3r'\, w(\vec{r}-\vec{r}';\bar{n}_i(\vec{r}))n_i(\vec{r}'). \tag{43}$$

The corresponding energy functional is

$$E_{\rm XC}\{n\} = \sum_i \int d^3r\, n_i(\vec{r})\epsilon_{\rm XC}(\bar{n}_i(\vec{r})). \tag{44}$$

Similarly, in the WDS approximation

$$E_{\rm XC}\{n\} = \frac{1}{2}\int d^3r\, n_i(\vec{r})\int d^3r'\, v(\vec{r}-\vec{r}')\Big(n_i(\vec{r}')G^h(\vec{r}-\vec{r}';\tilde{n}_i(\vec{r}))+\sum_{j\neq i} n_j(\vec{r})G^h(\vec{r}-\vec{r}';n(\vec{r}))\Big), \tag{45}$$

where $\tilde{n}_i(\vec{r})$ should be chosen so that the charge-conserving sum rule is satisfied. This will now take the form

$$-1 = \int d^3r'\Big(n_i(\vec{r}')G^h(\vec{r}-\vec{r}';\tilde{n}_i(\vec{r})) + \sum_{j\neq i} n_j(\vec{r})G^h(\vec{r}-\vec{r}';n(\vec{r}))\Big). \tag{46}$$

The usual shell division should be used: $1s$; $2s$, $2p$; $3s, 3p$; $4s, 4p, 3d$; etc. From an inspection of Eqs. (43)–(46) it is clear that the shell partitioning that we propose will cut off most of the unphysical inter-shell contributions to the AD and WD results.

IV. APPLICATIONS TO ATOMS

Calculations of various atomic properties have been performed in the local-density and local-spin-density (LSD) approximations by several authors.[3,4,8,21] These calculations show that, in particular, the LSD approximation gives rather good results for valence-electron properties like ionization potentials and electron affinities. On the other hand, the description of the core electrons is less adequate, and therefore the total energy results are not equally satisfactory. For instance, the error in the total exchange energy varies from about 14% for light atoms to about 5% for heavy atoms. The total energy of atoms is therefore a relevant property to calculate in order to illustrate the improvements brought about by the new nonlocal energy functionals.

We shall start by deriving some analytical results and then proceed to applying the AD and WD schemes to the exchange energy of atoms. We shall also illustrate the effects of the shell partitioning proposed in Sec. IIID. The exchange energy depends solely on the wave functions and is therefore more directly related to the electron density than is the correlation energy, which in addition depends on dynamic properties like the excitation spectrum.[22] One might anticipate therefore that the AD and WD schemes are particularly well suited for describing the exchange energy, whereas the correlation energy of atoms may be more difficult to improve upon. The above qualitative argu-

ments are borne out by numerical calculations, which will also be discussed. Finally, results for the total energy for a number of atoms are presented, and the XC potential is discussed.

As the aim of these atomic applications is merely to illustrate the virtues of the new approximations, complete self-consistent calculations have not been attempted. Rather, all calculations discussed here have been limited to evaluating the approximate XC functional in question using a density derived from the parametrized Hartree-Fock (HF) wave functions calculated by Clementi.[23]

A. Exact and asymptotic behaviors

The exact expressions for the XC energy density $\epsilon_{xc}(\vec{r})$ and potential $v_{xc}(\vec{r})$ simplify in the region far away from the nucleus. From Eqs. (15) and (17)–(19) it immediately follows that

$$\epsilon_{xc}(\vec{r}) \underset{r\to\infty}{\longrightarrow} -\tfrac{1}{2}(e^2/r). \tag{47}$$

This is due to the fact that when r is large the $\vec{r}'$ dependence of the factor $|\vec{r}-\vec{r}'|^{-1}$ of Eq. (14) may be neglected. [By large r is meant points $\vec{r}$ that lie outside the region, where $n(\vec{r}')$ is appreciable.] The sum rule of Eq. (18) then directly leads to Eq. (47).

Similarly, the exact XC potential as given by Eq. (9) has the asymptote

$$v_{xc}(r) \underset{r_s\to\infty}{\longrightarrow} -(e^2/r). \tag{48}$$

Here we have in addition used the fact that $\delta g(\vec{r}',\vec{r}'',\lambda)/\delta n(\vec{r})$ is zero in the above limit. This merely reflects the fact that an infinitesimal change of the density far from the nucleus cannot affect the pair correlations in the interior of the atom. We emphasize that the relation $v_{xc}(\vec{r}) = 2\epsilon_{xc}(\vec{r})$ implied by Eqs. (45) and (46) only holds for large values of r.

There is one application, for which one of the approximate functionals is the exact one: the hydrogen atom in the WD approximation. As $\int d^3r' n(\vec{r}') = 1$ in this one-electron system, and as the pair correlation function is non-negative, the sum rule Eq. (18) can be satisfied, only if $g^h_{\tilde{n}(\vec{r})}(\vec{r}-\vec{r}';\lambda) \equiv 0$ in Eq. (35), which gives $n^{WD}_{xc}(\vec{r},\vec{r}') = -n(\vec{r}')$, i.e., the exact result. This can be achieved by choosing $\tilde{n}(\vec{r}) \equiv 0$, i.e., the hydrogen atom is properly described by taking the pair correlation function from the homogeneous electron liquid in the Wigner-lattice limit!

Turning to the asymtotic behavior of the XC energy density and potential, it is clear that the LD approximation, due to its improper local-density prefactor in Eq. (16), is unable to produce the correct r^{-1} limit. Instead, both $\epsilon^{LD}_{xc}(\vec{r})$ and $v^{LD}_{xc}(\vec{r})$ go to zero exponentially for large r values.

The AD approximation [Eq. (20)] has a prefactor which through the averaging procedure of Eq. (21) has an indirect dependence on $\vec{r}'$. This is sufficient to produce the limiting r^{-1} dependence of $\epsilon_{xc}(\vec{r})$ and $v_{xc}(\vec{r})$, but their actual magnitude varies from atom to atom. This is illustrated for the XC energy density in Fig. 10, where we observe that for large r, $\epsilon^{AD}_{xc}(\vec{r})/(-e^2/2r)$ falls within 20% of the correct limiting value, which is unity.

The WD approximation [Eq. (35)] is defined with the correct density prefactor and obeys the sum rule [Eq. (18)], which ensures that the proper asymptotic limit for the exchange energy is obtained exactly[17] (cf. Fig. 10). We observe, however, that the WD, as well as the AD approximation, gives incorrect limits for the XC potentials. In both schemes $v_{xc}(\vec{r}) \to \epsilon_{xc}(\vec{r})$ rather than $2\epsilon_{xc}(\vec{r})$ for large r.

B. Exchange effects

The simplest system for illustrating exchange effects is the ground state of helium with just one electron of each spin. The exact exchange-energy

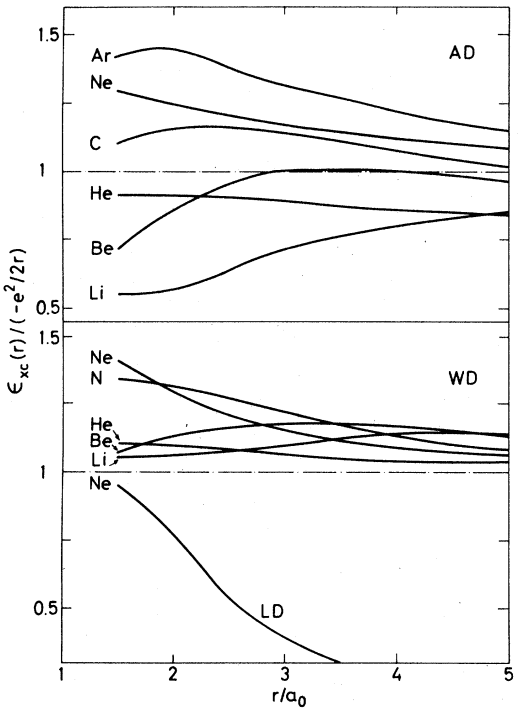

FIG. 10. Quantity $\epsilon_{xc}(r)/(-e^2/2r)$ for a number of atoms as a function of r in the AD and WD approximations. In a correct theory this quantity should tend to unity for large r. In the LD approximation it decays exponentially.

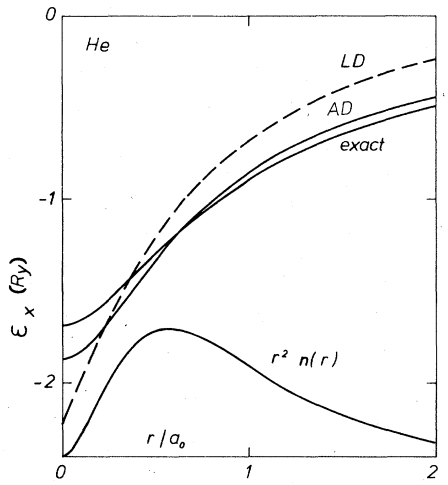

FIG. 11. Exchange-energy density $\epsilon_x(r)$ of helium as defined in Eq. (19) in the LD and AD approximations compared with the exact result Eq. (49). The WD approximation is exact in this case.

density for this system is

$$\epsilon_x(\vec{r}) = -\tfrac{1}{2}e^2 \int d^3r'\, n(\vec{r}')\Big/ |\vec{r}-\vec{r}'|\,. \tag{49}$$

In this particular case the exchange energy

$$E_x = \int d^3r\, n(\vec{r})\epsilon_x(\vec{r})\,, \tag{50}$$

can thus be expressed as a simple integral over the density.

We emphasize that we are using the term "exchange energy" as it is defined in the density-functional formalism. If we define the exchange energy as the difference between a Hartree-Fock (HF) and a Hartree calculation, it is clear that this is zero for the ground state of helium, as there is only one electron of each spin. However, in the density-functional formalism the exchange energy has to cancel an electrostatic term caused by the interaction of the electron with itself. It is this self-interaction that is cancelled exactly by Eq. (50) in the present case.

The helium atom in its ground state with only exchange effects considered, happens to be another case where the WD approximation is exact. The reason is that in a spin-compensated two-electron system there is no other electron to exchange with, and the result follows from arguments analogous to those used for the hydrogen atom in Sec. III.

The exact and approximate exchange-energy densities $\epsilon_x(\vec{r})$, evaluated as described in the introduction of this section are shown in Fig. 11. As mentioned above, the WD approximation gives the exact result in this particular case and requires no further discussion. To appreciate the improvements over the LD approximation furnished by the AD scheme, consider first the point $\vec{r}=0$. In the LD approximation the surrounding density is assumed equal to the local one $[n(\vec{r}=0)]$, which is an overestimate. The LD approximation therefore gives too strong exchange effects, and $\epsilon_x(\vec{r}=0)$ is too negative. The average density used in the AD approximation has to be lower than $n(\vec{r}=0)$, and $\epsilon_x(\vec{r}=0)$ is therefore raised. This reduces the error for $\vec{r}=0$ by a factor of 3. For large r the situation is the opposite. The local density is smaller than the density in the surroundings of the nucleus. Thus, the LD result for $\epsilon_x(r)$ is not sufficiently negative. In the AD scheme, however, the use of an average density takes the higher density in the neighborhood of the nucleus into account and it brings the curve close to the exact one.

In Table III we give results for the exchange energy of some other atoms. Here we have used a spin-polarized spin-density-functional (SDF) formalism for the LD and WD calculations. In the AD scheme we added the lowering of the energy due to spin polarization that is obtained in the LD approximation. This is of little importance for the total energies, except for the lightest atoms. The generalization of the WD scheme to account for spin polarization, when only exchange effects are included, is straightforward,[17] and follows from simply letting the shell indices in Eqs. (45) and (46) also contain a spin index.

The improvements over the LD approximation are striking, especially for light atoms. The less drastic improvement for heavier atoms is mainly

TABLE III. Exchange energy in rydbergs of some spherically symmetric atoms using the LSD approximation and the nonlocal functionals named AD, ADS, WD, and WDS (see text), compared with the exact HF result. The numbers in parentheses are errors in percent.

	LSD	AD	ADS	WD	WDS	Exact
He	−1.768(13.8)	−2.056(0.2)	−2.056(0.2)	−2.052(0.0)	−2.052(0.0)	−2.052
Li	−3.08(13.5)	−3.66(2.8)	−3.55(0.3)	−3.57(0.3)	−3.54(0.6)	−3.56
Be	−4.63(13.1)	−5.53(3.8)	−5.32(0.2)	−5.38(0.9)	−5.31(0.4)	−5.33
N	−11.79(10.6)	−13.75(4.2)	−13.27(0.6)	−13.68(3.7)	−13.37(1.4)	−13.19
Ne	−22.07(8.9)	−25.08(3.6)	−24.55(1.4)	−25.59(5.7)	−24.87(2.7)	−24.22
Mg	−29.22(8.7)	−33.14(3.6)	−32.29(0.9)	−33.98(6.2)	−32.72(2.3)	−31.99

due to an overestimate in the AD and WD schemes of the intershell contribution, as discussed in Sec. IIID.

Table III indicates that the AD and WD approximations are of comparable accuracy. This might at first be somewhat surprising, considering that the XC hole should be substantially better reproduced in the WD approximation. In particular, if only exchange effects are included, the WD approximation gives the correct result for $n_x(\vec{r},\vec{r}')$ in the limit $\vec{r}\to\vec{r}'$. Furthermore the WD approximation includes some of the asymmetry of the XC hole. For instance, even when the electron is far from the nucleus, the hole remains in the atom, while in the AD approximation the hole is always spherically symmetric around the electron. These points are, however, not very important for the XC functional, which is the only quantity needed in the solution of the SDF equations. There are at least two reasons for this. First, the limit $\vec{r}\to\vec{r}'$ of $n_{XC}(\vec{r},\vec{r}')$ is of little importance in Eq. (14), due to the volume element. Second, the functional (14) depends only on the spherical average $n_{XC}^{SA}(\vec{r},r'')$ [Eq. (17)], and therefore an improved description of the nonspherical parts of $n_{XC}(\vec{r},\vec{r}')$ does not improve the functional.

Table III shows that there is a considerable improvement in the exchange energy, when including the shell-partitioning procedure (ADS and WDS).[17] That this is not due to some cancellation of errors but entirely due to the mechanisms described in Sec. IIID, can be illustrated by a detailed study of the exchange-energy density $\epsilon_x(r)$ for a typical atom. This is possible, as the exact $\epsilon_x(r)$ can be calculated by using Clementi's[23] Hartree-Fock spin orbitals $\Psi_{io}(r)$ in Eq. (42).

In Fig. 12, which shows the quotient $\epsilon_x(\vec{r})/\epsilon_x^{exact}(\vec{r})$ for the neon atom, we observe (a) how the misrepresentation of the LD approximation is reduced considerably by the AD and WD approximations not only for small- and large-r values, in the same way as discussed earlier for He, but also for most intermediate-r values, (b) that the remaining errors of the AD and WD are largest in the region between the valence- and core-electron shells, and (c) that the ADS and WDS approximations reduce these errors significantly. The shell partitioning is thus a systematic way of improving the description of the intershell exchange effects.

C. Exchange and correlation

In the Kohn-Sham scheme, the XC effects are naturally treated together. Table IV gives the XC energy of a few atoms as calculated in the AD and WD schemes. Let us examine the AD results first. We observe that the XC energy is again considerably improved compared to the LD approximation. Thus the error in the LD approximation

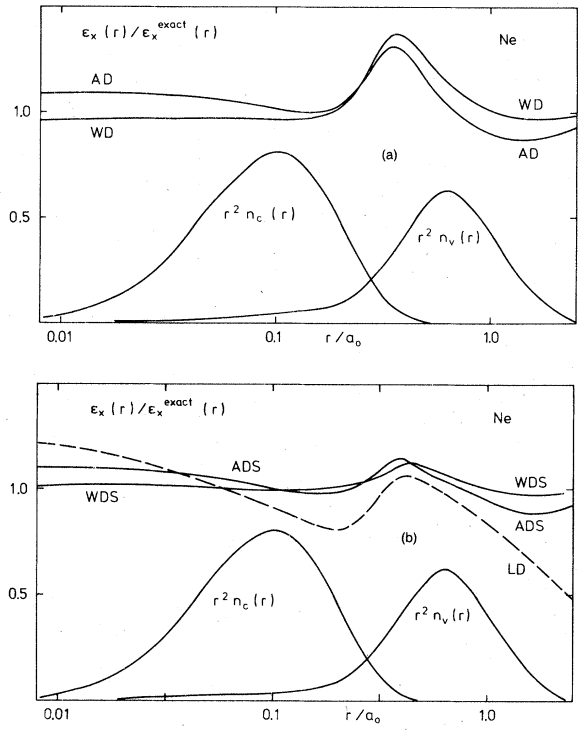

FIG. 12. Quotient $\epsilon_x(r)/\epsilon_x^{exact}(r)$ for a neon atom, where $\epsilon_x^{exact}(r)$ is calculated from Eq. (42) by using the Hartree-Fock spin-orbitals of Clementi (Ref. 23). The electron density in the core and valence shells are denoted by $n_c(r)$ and $n_v(r)$, respectively. In (a) results are given for the AD and WD approximations while in (b) the shell partitioning described in Section III D has been used to give the ADS and WDS curves. The dashed curve shows the result in the LD approximation.

is about (5–8)%, while in the AD approximation it varies from about 2% for light atoms to less than 1% for heavy atoms. With the shell partitioning the error is on the average further reduced, but the reduction is not as significant as when only the exchange energy was considered.

On closer inspection it is clear that this is due to a rather poor account of the correlation energy in the AD scheme. Still, the ADS scheme significantly improves the exchange-correlation energy for a large number of atoms, as is illustrated in Fig. 13.

The WD results of Table IV are less encouraging.[24] They overestimate the magnitude of E_{XC} with almost the same amount as the LSD approximation underestimates E_{XC}. If we were to define the correlation energy by simply subtracting the E_x values of Sec. IV B, we would find that the magnitude of the correlation energy is a factor of 2 to 3 too small in the AD approximation, while in the LSD and WD approximations it is roughly a factor of 2 to 3 too large.

Only a minor part of the overestimation of the

TABLE IV. Exchange-correlation energies in rydbergs for some spherically symmetric atoms. The "exact" experimental correlation energies were obtained by Clementi [a] by correcting for estimated relativistic effects not included in our calculations. In the WDS approximation the RPA has been used to calculate $G(q, r_s)$ [Eq. (38)]. The numbers in parentheses are the errors in percent.

	LSD	AD	ADS	WD	WDS	Exact
He	−2.00(6.5)	−2.06(3.7)		−2.49(17)		−2.14
Li	−3.37(7.7)	−3.59(1.6)	−3.51(3.8)	−4.19(15)	−4.16(14)	−3.65
Be	−5.09(8.6)		−5.36(3.8)	−6.23(12)	−6.16(11)	−5.57
N	−12.44(8.3)	−13.24(2.4)	−13.17(2.9)	−14.54(7.1)	−14.39(6.0)	−13.57
Ne	−23.56(5.8)	−25.47(1.8)	−24.86(0.6)	−26.94(7.7)	−26.65(6.6)	−25.01
Ar	−58.56(5.4)	−62.47(0.9)	−61.39(0.8)	−66.20(6.9)	−64.66(4.4)	−61.91
K	−63.35(5.4)	−67.52(0.9)	−66.37(0.9)	−71.60(6.9)		−66.94

[a]Reference 24.

correlation energy in the WD scheme could be due to the use of the RPA for $G(q, r_s)$ in Eq. (37). The local densities in atoms are quite high ($r_s \lesssim 1$), and in this regime the RPA should be a reasonable approximation. To support this argument we can mention that using the Hubbard approximation rather than the RPA reduced the XC energy of He from −2.49 to −2.40 Ry and the error in $E_{\rm XC}$ from 17% to 13%.

We end this section by illustrating in Table V, how the ADS results will improve the total energy of a number of atoms. As the difference between the XC energies calculated in the ADS and LSD approximations, respectively, is so small compared to the total energy, first-order perturbation theory may be used to calculated the total energy in the ADS scheme. This means that we add the difference in XC energy ($E^{\rm XC}_{\rm ADS} - E^{\rm XC}_{\rm LD}$) to the total energy $E_{\rm LD}$ calculated in a self-consistent LD calculation. As for the spin polarization, we assume this small effect to be similar in the LD and ADS schemes and add a term ($E^{\rm XC}_{\rm LSD} - E^{\rm XC}_{\rm LD}$) to get

$$E_{\rm ADS} \simeq E_{\rm LSD} + (E^{\rm XC}_{\rm ADS} - E^{\rm XC}_{\rm LSD}). \quad (51)$$

The above procedure obviously gives the exact result provided $E_{\rm exact} - E_{\rm LSD} = E^{\rm XC}_{\rm ADS} - E^{\rm XC}_{\rm LD}$. As can be seen from Table V, the ADS approximation reduces the error in the total energy by a substantial fraction, ranging from about 50% for light atoms to about 90% for heavy atoms.

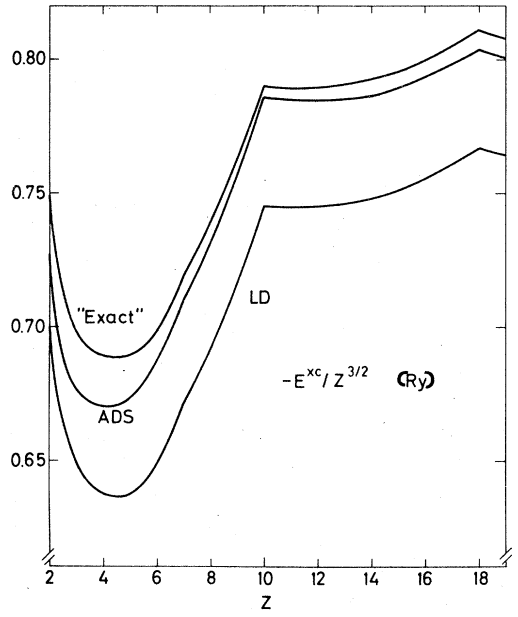

FIG. 13. Atomic XC energy in the ADS and LD approximations compared to the quantity $E^{\rm XC}_{\rm LD} + (E_{\rm exp} - E_{\rm LSD})$ which is here considered to be the "exact" result. The experimental result $E_{\rm exp}$ has been corrected by Clementi (Ref. 24), for estimated relativistic effects not included in the present calculations. The energies have been divided by $Z^{3/2}$ to get a roughly Z-independent quantity (Z is the charge of the nucleus).

TABLE V. Total energies in rydbergs for a number of atoms. The exact results are taken from Clementi [a]. The difference between the exact result and the result of a self-consistent LSD calculation is compared with the difference between the exchange-correlation energy, calculated in the ADS and LD schemes, respectively.

	$-E_{\rm LSD}$	$-E_{\rm exact}$	$E_{\rm exact} - E_{\rm LSD}$	$E^{\rm XC}_{\rm ADS} - E^{\rm XC}_{\rm LD}$
He	5.6798	5.8076	−0.13	−0.05
Li	14.7066	14.9560	−0.25	−0.14
Be	28.9088	29.3348	−0.43	−0.27
B	48.7248	49.308	−0.58	−0.41
C	74.9598	75.6932	−0.73	−0.57
N	108.2936	109.1778	−0.88	−0.73
O	149.0682	150.1348	−1.07	−0.91
F	198.2368	199.466	−1.23	−1.10
Ne	256.4691	257.880	−1.41	−1.29
Na	322.8982	324.5238	−1.63	−1.46
Mg	398.272	400.1272	−1.86	−1.64

[a]Reference 24.

D. Exchange-correlation potential

As described in the introduction of this section nonlocal effects have only been evaluated for the XC energy E_{xc}. Although we believe this to be the leading effect, the XC potentials are given by well-defined expressions in the AD [Eqs. (33) and (34)] and WD approximations [Eqs. (40) and (41)], and may be readily calculated. It is mainly our desire to keep this article down to a reasonable size that has made us postpone this task for a future publication. The nonlocal aspects of $v_{xc}(\vec{r})$ are certainly worth a study of their own.

In this context it is particularly interesting to draw our attention to the conceptual problem encountered for the negative hydrogen atom H^- treated in the LD approximation.[25] Here the XC potential far from the nucleus tends to zero exponentially, and therefore, due to the electron self-interaction, the potential far from the nucleus is $2(e^2/r)+(-e^2/r)$, i.e., positive. In fact the energy eigenvalue ϵ_i in the Kohn-Sham equation is positive and the corresponding eigenfunction is not normalizable. To remedy this unphysical result a nonlocal XC potential is needed which has to cancel the term e^2/r that is due to the electron self-interaction. However, preliminary results[26] indicate that with the present implementation of the AD and WD approximations a positive eigenvalue is retained. Improved XC potentials might be obtained if the replacement of the pair-correlation function, $g \to g^h$, is made in the *exact* expression for $v_{xc}(\vec{r})$ derived from Eqs. (9) and (14). With this procedure the exact result $v_{xc}(\vec{r}) = 2\epsilon_{xc}(\vec{r})$ for $\vec{r}$ far from the nucleus could be retained.[27]

When it comes to a practical computational scheme, the scope of this article, however, the improvements in $v_{xc}(\vec{r})$ and thus in the density $n(\vec{r})$ are of secondary importance. This is due to the demonstrated relative insensitivity of the total energy to density changes.[1]

V. APPLICATON TO SURFACES

The surface region of metals has a strongly varying electron density. At the same time, because the metal is an extended system, a surface represents a very different kind of inhomogeneity than does an atom. It is a demanding task for any approximate description of exchange and correlation to suit both systems equally well.

In this section we shall study the virtues and limitations of the AD and WD approximations in the semi-infinite jellium model of surfaces. In this model, which has been used in a wide variety of surface problems,[28,29] the valence electrons are moving in the potential of a semi-infinite, uniform positive background charge. The application of the AD and WD schemes to this model surface will be found only partially successful. Outside the metal, the XC potential and energy density appear to be considerably better described in these approximations than in the local density (LD) approximation. On the otner hand, inside the metal the shape of the XC hole appears to be too approximate. To be specific, for an electron at a point z in the metal, say, a few screening lengths from the surface, the exact XC hole differs from the bulk hole only *in the surface region*, while the approximate AD and WD holes show small but significant deviations also *inside the metal.* This is only a slight misrepresentation and has no influence on $\epsilon_{xc}(\vec{r})$ and $v_{xc}(\vec{r})$ which take the proper bulk-limit values. However, for a semi-infinite system the effect on integrated quantities such as the XC part of the surface energy may be large. As we shall see, this is indeed the case.

To illustrate these points, it suffices to calculate the metal surface properties using the electron density of the so-called infinite-barrier model (IBM),[30]

$$n(z) = n_0\left[1 + 3\left(\frac{\cos(2k_F z)}{(2k_F z)^2} - \frac{\sin(2k_F z)}{(2k_F z)^3}\right)\right]\Theta(-z), \quad (52)$$

where $k_F = (3\pi n_0)^{1/3}$ is the Fermi wave vector corresponding to the bulk density n_0. The IBM has well-known shortcomings. It contains, for instance, only one length k_F^{-1} and therefore the width of the surface region is proportional to k_F^{-1} rather than to the screening length. For bulk densities corresponding to $r_s = 4-5$, however, the two lengths are roughly equal, and the IBM models quite well[30] the electron density obtained in more realistic calculations.[31] In addition, with this procedure the electron density will not be self-consistently calculated. The XC energy density and potential have therefore also been evaluated in the semiclassical infinite-barrier model (SCIBM),[32] where

$$n(z) = n_0\Theta(-z). \quad (53)$$

We have found that these quantities are remarkably insensitive to even such a drastic change in the density profile. The reason for this is, of course, the averaging procedure inherent in the nonlocal density dependence of the AD and WD approximations.

A. Exact and asymptotic behaviors

At points far outside the surface (large z), the exact XC energy density and potential go over into the proper image-potential behavior,

$$\epsilon_{xc}(\vec{r}) \to -e^2/4z \quad \text{for } z \to \infty \quad (54)$$

and

$$v_{\rm XC}(\vec{r}) \to -e^2/4z \quad \text{for } z \to \infty . \tag{55}$$

This can be seen from Eqs. (9), (14), (15) and (18) by letting $\vec{r}=(x,y,z)$ grow large enough to make the limiting case of a point charge outside a grounded conductor applicable. Then the XC hole is smeared out over the surface, or in the method of images effectively localized at $(x,y,-z)$, i.e., at a distance of $2z$ from the electron at $\vec{r}=(x,y,z)$. The pair-correlation function $g_n(\vec{r},\vec{r}';\lambda)$ in Eq. (15) expresses the conditioned probability to find an electron at $\vec{r}'$, *if* there is one at $\vec{r}$, and in the general case these are correlations between indistinguishable electrons. For large z, however, the electron at $\vec{r}$ acquires an identity and therefore the correlations are the same as for a classical point charge. Thus the classical image argument applies. [The argument about g, the pair-correlation function, becomes particularly apparent in the Hartree-Fock approximation, where $g_n(\vec{r},\vec{r}';\lambda)$ does *not* depend on the interaction between the electrons. The coordinate $\vec{r}'$ of Eq. (14) will then run over the whole semi-infinite metal, replacing the limiting forms Eqs. (54) and (55) by zero to order $1/z$ when only exchange effects are included.]

A major deficiency of the LD approximation is that it is unable to give the image-force behavior. Instead it gives an XC energy density and potential that decay exponentially outside the surface,[5] as does the local density.

The imagelike form of $v_{\rm XC}(\vec{r})$ in the WD approximation can be derived from Eqs. (39)–(41). The first and second terms of Eq. (40) differ only by their density arguments, being $\bar{n}(\vec{r})$ and $\bar{n}(\vec{r}')$, respectively. For points $\vec{r}$ far outside the surface, however, this difference is crucial, as it implies that $w_{\rm XC}^{\rm WD}(z)$ tends to $\epsilon_{\rm XC}^{\rm WD}(z)$ in this limit. This we conclude by noting that the factor $n(\vec{r}')G^h(|\vec{r}-\vec{r}'|;\bar{n}(\vec{r}'))$ of the last two terms in Eq. (40) is nonzero only for points $\vec{r}'$ inside the metal. On the other hand, for these $\vec{r}'$, the range of the function G is roughly equal to $[\bar{n}(\vec{r}')]^{1/3}$ where $\bar{n}(\vec{r}') \simeq n_0$. Thus $G^h(|\vec{r}-\vec{r}'|;\bar{n}(\vec{r}'))$ tends to zero as $|\vec{r}-\vec{r}'|$ gets large, and therefore $\epsilon_{\rm XC}^{\rm WD}(z)$ and $v_{\rm XC}^{\rm WD}(z)$ have the limiting form $-e^2/2z$. Apparently the WD potential and energy density both come out twice too large in this limit.

Actually, the $-e^2/2z$ form is obtained only if $g^h(r)$ vanishes faster than any inverse power of r for large $\vec{r}$. Otherwise the center of gravity of the XC hole will not remain in the surface region, and the argument that allows us to replace $v(\vec{r}-\vec{r}')$ by $v(r)$ in Eq. (39) will not go through, which in turn leads to a different limit for $\epsilon_{\rm XC}^{\rm WD}$. If, for instance, we consider exchange effects only, i.e., use the Hartree-Fock version, $g^{\rm HF}(r)$, of the pair correlation function, which vanishes only as r^{-4} for large r,[33] we find that $\epsilon_{\rm XC}^{\rm WD} \to -e^2/6z$.

By repeating the previous discussion about $n(\vec{r})G^h(\vec{r}-\vec{r}';\bar{n}(\vec{r}'))$ for $n(r')w(\vec{r}-\vec{r}';\bar{n}(\vec{r}'))$ in Eqs. (33) and (34) one finds that also in the AD approximation $v_{\rm XC}^{\rm AD}(z) \to \epsilon_{\rm XC}^{\rm AD}(z)$ far outside the metal. As we know $w(r,\bar{n})$ only numerically, we cannot extract an exact analytical limit. However, as the range of $w(r,\bar{n})$ is approximately $(\bar{k}_F)^{-1} \simeq 0.5\bar{r}_s$, Eq. (21) implies that $\bar{r}_s$ should roughly equal $2z$. On using, for instance, Wigner's formula for the correlation energy of a low-density homogeneous electron gas[34]

$$\epsilon_{\rm xc}^{\rm AD}(\bar{n}) = [-0.916/\bar{r}_s - 0.88/(\bar{r}_s+7.8)]_{\bar{r}_s=2z} \ \text{Ry} ,$$

in Eq. (22), one finds that

$$\epsilon_{\rm xc}^{\rm AD} \to -1.8/2z \ \text{Ry} \simeq -e^2/2z ,$$

which is approximately the same limiting result as in the WD scheme.

On the bulk side, i.e., for $z \to -\infty$ both the WD and AD approximations give the correct bulk limits for $\epsilon_{\rm XC}(z)$ and $v_{\rm XC}(z)$. For points $\vec{r}$ far inside the metal, namely, $n(\vec{r})$ may be replaced by n_0, the constant bulk density. It then follows from Eqs. (36) and (39)–(41) that $\bar{n}(r) \to n_0$,

$$\int d^3r'\, G^h(\vec{r}-\vec{r}';\bar{n}) \to 1/n_0$$

and

$$\int d^3r'\, v(\vec{r}-\vec{r}')G^h(\vec{r}-\vec{r}';\bar{n}) \to \frac{2\epsilon_{\rm XC}^{\rm bulk}}{n_0}.$$

According to Eqs. (39)–(41) then clearly $\epsilon_{\rm XC}^{\rm WD}(z) \to \epsilon_{\rm XC}^{\rm bulk}$ and

$$v_{\rm XC}^{\rm WD}(z) \to v_{\rm XC}^{\rm bulk} = \frac{d[n_0\epsilon_{\rm XC}^{\rm bulk}(n_0)]}{dn_0}$$

for $z \to -\infty$. The AD approximation gives the proper bulk limits in the same way, as Eq. (21) implies that $\bar{n}(\vec{r}) \to n_0$ for $z \to -\infty$.

B. Numerical results

In the surface region, the region of prime interest, $\epsilon_{\rm XC}$ and $v_{\rm XC}$ have to be calculated numerically. In the WD approximation this amounts to solving Eq. (36) for $\bar{n}(\vec{r})$, here using the electron density Eq. (52) and the RPA [Eq. (38)] for G. In the AD scheme we have to solve Eq. (21) for $\bar{n}(\vec{r})$. Once $\bar{n}(\vec{r})$ or $\bar{n}(\vec{r})$ is known, it is in principle straightforward to calculate the XC energy density and potential from, respectively, Eqs. (39)–(41) and (22), (33), and (34). For the semi-infinite jellium problem, however, the fairly complicated expressions for the potentials may be reasonably approximated as follows (see Appendix D):

$$v_{\rm XC}^{\rm WD}(\vec{r}) \simeq \epsilon_{\rm XC}^{\rm WD}(\vec{r}) + \frac{1}{2}\int d^3r'\, n(\vec{r}')v(\vec{r}-\vec{r}')G^h(\vec{r}'-\vec{r};n_0) + \left(\epsilon_{\rm XC}^{\rm bulk}(n_0) - n_0\frac{d}{dn_0}\epsilon_{\rm XC}^{\rm bulk}(n_0)\right) \times \int d^3r'\, n(\vec{r}')G^h(\vec{r}-\vec{r}';n_0)\,, \quad (56)$$

and

$$v_{\rm XC}^{\rm AD}(\vec{r}) \simeq \epsilon_{\rm XC}^{\rm AD}(\vec{r}) + \left(\frac{d}{dn_0}\epsilon_{\rm XC}^{\rm bulk}(n_0)\right) \times \int d^3r'\, n(\vec{r}')w(\vec{r}-\vec{r}';n_0)\,. \quad (57)$$

These equations have the same limiting form as the original expressions Eq. (33) and (40), respectively, and are quite accurate also in the surface region.

The XC potentials for three different bulk densities calculated in the above manner in the WD approximation are displayed in Fig. 14. We note that the potentials smoothly go over from the bulk (RPA) potential to an imagelike behavior. In Fig. 15 we show the XC potential calculated in various schemes, for a bulk density corresponding approximately to aluminum ($r_s = 2$). As is indicated in Fig. 15, the AD approximation, too, gives an XC potential that interpolates between the bulk value and an imagelike limit. Apparently, the AD curve reaches its asymptotic form rather close to the surface, while the WD curve stays quite close to the true image potential for intermediate-z value. The LD approximation of course gives an XC potential that is zero outside the infinite barrier, where the electron density vanishes.

The WD scheme in connection with the SCIBM electron density of Eq. (53) would have given a curve in Fig. 15, hardly distinguishable from the IBM one. It is interesting to note that even for such a drastic difference in electron density profile, the change in $v_{\rm XC}^{\rm WD}$ is minute.

C. Surface energy

The surface energy is an integral property that expresses the energy cost upon creating a new surface. The XC part of the surface energy, $\sigma_{\rm XC}$, is in the jellium model related to the XC energy density in the following way[28]:

$$\sigma_{\rm XC} = \int_{-\infty}^{\infty} dz\, n(z)[\epsilon_{\rm XC}(z) - \epsilon_{\rm XC}^{\rm bulk}(n_0)]\,. \quad (58)$$

The integrand of Eq. (58) is shown in Fig. 16 for the WD and LD approximations applied to the IBM electron density Eq. (52). Close to the surface we find the expected result of the nonlocal density dependence, i.e., a raise compared to the LD result

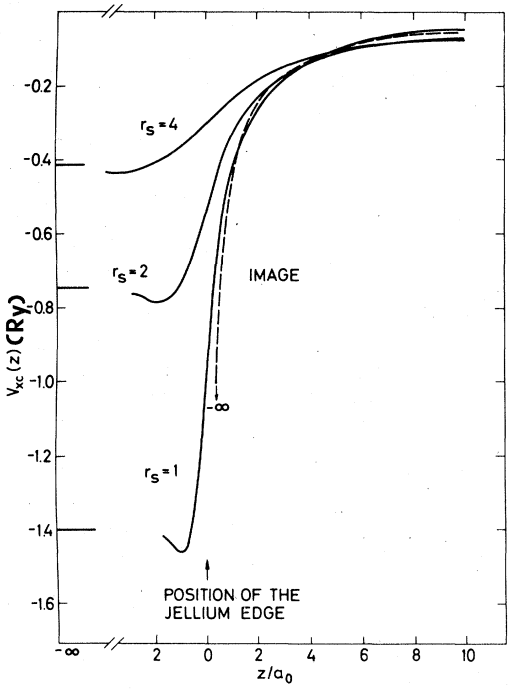

FIG. 14. XC potential in the WD approximation for the infinite-barrier model of a metal surface. Results are given for three different bulk densities corresponding to $r_s = 1, 2$, and 4. The image potential ($-e^2/4z$) is given by the dashed curve.

outside the surface and a decrease just inside. Further inside the metal, the LD curve oscillates around zero, reflecting the oscillations in the electron density $n(z)$ of Eq. (52). Although the WD curve also oscillates, the mean value lies below the x axis. This is a common feature of both the XC energy density $\epsilon_{\rm XC}^{\rm WD}(z)$ and potential $v_{\rm XC}^{\rm WD}(z)$ in the WD approximation. The reason for this behavior can be understood as follows: Consider the equation that determines $\tilde{n}(\vec{r})$, i.e., Eq. (36), for a point $\vec{r} = (x, y, z)$ well inside the metal. Clearly, the difference between the XC hole $n_{\rm XC}^{\rm WD}(\vec{r}, \vec{r}')$ and the bulk hole $n_{\rm XC}^{\rm bulk}(\vec{r}, \vec{r}')$ is that a small amount of charge from the region outside the surface is removed and distributed over the rest of the hole. In effect, a small amount of charge, $-e\Delta n$, is moved from a distance $|z|$ to a distance $r_s^{\rm bulk} < |z|$ from the center of the XC hole. The contribution to $\sigma_{\rm XC}$ from the point $\vec{r}$ will therefore be $e^2 n_0 \Delta n(-1/r_s^{\rm bulk} + 1/|z|) < 0$. Now, in an exact theory, we expect the XC hole centered around a point well inside the metal to differ from the bulk hole only in the surface region. The contribution to the surface energy should accordingly be proportional to $n_0\Delta n/|z|$. Several screening lengths inside the metal Δn will go to zero and so will therefore the integrand of Eq. (58).

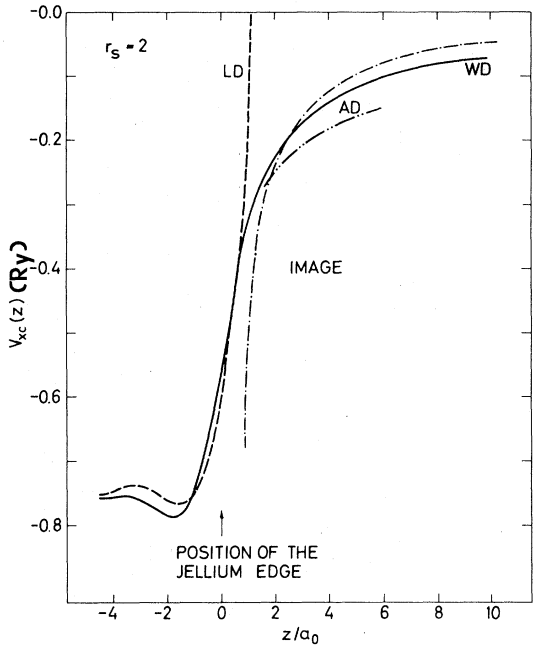

FIG. 15. XC potential for the infinite-barrier model of a metal surface. The bulk density corresponds to $r_s = 2$. Results are given for the WD (full curve) and LD approximations (dashed curve) (these are calculated using data for the homogeneous electron gas given by the RPA) as well as for the AD approximation (dashed–double-dotted curve). The dash-dotted curve gives the image-potential $(-e^2/4z)$. To avoid congestion of the figure we show the AD result only outside the surface. In the surface region the AD and WD results are similar.

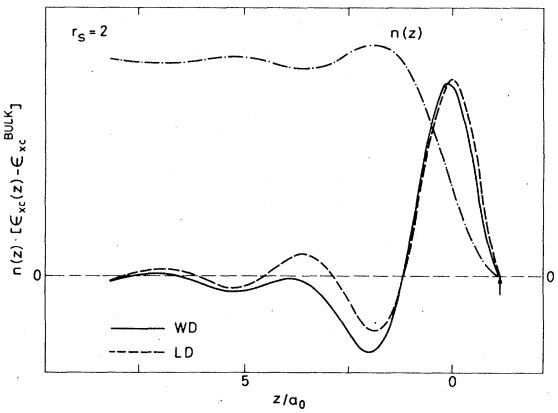

FIG. 16. Surface XC energy density, i.e., the integrand of Eq. (58) for the infinite-barrier model. The jellium edge is at $z = 0$ and the position of the infinite barrier is indicated by an arrow. The full curve shows the result of the WD approximation, the dashed curve gives the result in the LD approximation. The dash-dotted curve indicates the electron density in the infinite barrier model. The bulk density corresponds to $r_s = 2$.

This point, however, requires a small digression: If only exchange effects (i.e., the Pauli principle) are included in the pair correlation function $g(r)$, Δn vanishes only as $1/|z|$ and accordingly σ_x^{WD} diverges. As soon as correlations are taken into account Δn vanishes faster and the integral Eq. (58) converges. Still, even in this case the deficiency of the WD approximation as described above is of numerical importance and leads to a poor value for the XC contribution to the surface energy, as can be seen for the IBM in Table VI.[35,36]

In the AD approximation scheme the XC hole is misrepresented in much the same way. In fact $\epsilon_{XC}^{AD}(z)$ tends so slowly towards its bulk value that the contributions from far inside the metal to σ_{XC} is unreasonably large. We shall therefore not quote any numerical results here but refer to Appendix E for a discussion.

D. Discussion

The surface applications illustrate several virtues and vices of the AD and WD approximations. For the XC energy density and potentials the schemes give an overall very reasonable modelling. Like the LD approximation the proper bulk limits are retained deep inside the solid, but unlike the LD approximation both the AD and WD schemes in addition give an image behavior far outside the surface. In approaching the bulk value, there is inside the surface a slight misrepresentation of the XC hole. This has only minor effects of lowering the $v_{XC}(\vec{r})$ and $\epsilon_{XC}(\vec{r})$ values inside the surface. For certain quantities, like the surface energy contribution σ_{XC} discussed in Sec. VC, the misrepresentations might integrate up to erroneous results. For the surface energy this occurs because a difference between an infinite and a semi-infinite system is taken.

To avoid such consequences, surface applications of the AD and WD approximations should be limited to situations, where errors due to the slight misrepresentation of the XC hole are not summed up but rather cancel in a systematic way. The schemes should be most useful in describing differences in energies, for instance, in the chemisorption problem, where only adsorbate-induced effects are considered, or where energy differences between various adsorption sites are of interest.

VI. CONCLUSIONS

In this paper, which is devoted to extensions of the Kohn-Sham density functional scheme beyond the local-density (LD) approximation, we have criticized the earlier proposed gradient expansion

TABLE VI. Exchange-correlation surface energy in ergs/cm^2 in the RPA approximation to the IBM model. WD denotes the result of the present work, LD the local-density approximation and Exact is the Inglesfield-Wikborg result[a] as modified by Langreth and Perdew[b].

r_s	WD	LD	Exact
1	3520	10700	...
2.07	585	1240	1388
4	102	184	203

[a]Reference 35. [b]Reference 36.

[Eq. (2)] and density-response-kernel techniques [Eq. (3)]. As alternatives, we propose two new functional forms for the exchange-correlation (XC) energy,[38] which both use data for the homogeneous electron liquid as input but in a more intricate way than the LD approximation. These "average-density" (AD) and "weighted-density" (WD) approximations (a) go over into the LD approximation in the homogeneous limit, (b) have a nonlocal dependence on the electron density, through a physical weighting of the densities in the surroundings, and (c) satisfy a sum rule for the XC hole that ensures charge conservation. The two approximations differ only in the way the averaging or weighting is performed. In principle, the proposed functionals generate XC potentials according to Eq. (9), and then the density should be obtained by self-consistantly solving Eqs. (5)–(9).

The practical procedure that we suggest for applications is the same as was followed here, i.e., first to perform a self-consistent calculation of the electron density $n(\vec{r})$ in a simple scheme, e.g., the LD approximation, and then to proceed to a final evaluation of the total energy in the AD or WD approximations using this density. In computational programs for atoms, molecules, and solids based on local potentials, the additional amount of programming as well as computing time is then small as the self-consistency procedure can be left unchanged and only the last part of the Kohn-Sham calculation, the evaluation of the total energy, has to be modified.

It is of course desirable that the approximate XC functional is generally applicable. In explicit applications on two widely different electron systems, atoms and metallic surfaces, we have examined the virtues and vices of the AD and WD approximations. In several aspects there is a considerable improvement upon the LD approximation: the r^{-1} behavior of $\epsilon_{xc}(\vec{r})$ and $v_{xc}(\vec{r})$ in the outskirts of atoms, the z^{-1} behavior of the same quantities far outside the metal surface, and the substantially improved total-energy values of atoms, particularly in the AD approximation. On the other hand, the coefficients of the asymptotic form are exact only in the WD approximation and for $\epsilon_{xc}(\vec{r})$ of atoms, and the improvement in total energy values upon the LD approximation is not as significant with both exchange and correlation effects included as when only exchange is considered.[16,17] This is a stringent test, however, as the calculations include both core and valence electrons. In a situation, where only valence electrons are studied, the modeling of XC effects by using data from the homogeneous electron liquid should be much more appropriate. In particular, this should be true for band-structure calculations for metals where the excitation spectrum is almost as continuous as for the homogeneous electron liquid.

The greatest vice of the AD and WD approximations found so far is the bad result for the surface energy of metals. This is due to a slight misrepresentation of the XC hole inside the surface, which upon the integrated comparison with the bulk hole sums up to an essential error. The lesson to learn for other applications to semi-infinite systems is that they have to be arranged so that the small systematic errors due to the XC hole misrepresentation cancel rather than add. Thus proper differences should be calculated. For instance, in a chemisorption calculation, the adsorbate-induced effects should be calculated by subtracting the result for the semi-infinite clean substrate from that of the combined subtrate plus adsorbate.

ACKNOWLEDGMENT

This research has been supported in part by the Swedish National Science Research Council.

APPENDIX A

This appendix contains a discussion of the exchange-correlation (XC) energy of an atom as obtained by employing the expansion of the XC energy functional to second order in the density variations. For a spherically symmetric system such an expansion yields [cf. Eq. (3)]

$$E_{xc}\{n\} = \int d^3r\, n(r)\epsilon_{xc}(n(r)) - 2\pi^2 \int_0^\infty r^2\,dr \int_0^\infty r'^2\,dr' \int_0^\pi d\theta \sin\theta\, K_{xc}\{|\vec{r}-\vec{r}'|, n\}[n(r)-n(r')]^2, \quad \text{(A1)}$$

where θ is the angle between $\vec{r}$ and $\vec{r}'$.

We wish to demonstrate that the integral over the kernel $K_{xc}\{r,n\}$ in (A1) gives an *infinite* contribution to the XC energy, if the density argument n is chosen to be (a) $n(\frac{1}{2}(\vec{r}+\vec{r}'))$ or (c) $n(\frac{1}{2}(|\vec{r}|+|\vec{r}'|))$ but a *finite*

contribution if (b) $n=\frac{1}{2}[n(\vec{r})+n(\vec{r}')]$ is used.

The substitution $y=|\vec{r}-\vec{r}'|$ in the second term, ΔE_{xc}, of (A1) gives

$$\Delta E_{xc}=-4\pi^2\int_c^\infty r\,dr\int_0^\infty r'\,dr'\int_{|r'-r|}^{r'+r} y\,dy\,K_{xc}(y,n)[n(r)-n(r')]^2. \tag{A2}$$

The convergence of (A2) depends on the kernel K_{xc} and it is useful at this stage to introduce the approximation

$$K_{xc}\{y,n\}\approx k_F(n)f\{yk_F(n)\}, \tag{A3}$$

which is exact if only exchange effects are included. However, numerical values of K_{xc} for metallic densities suggest that this form is a good approximation, even when correlation is included, the small deviation certainly not affecting the convergence properties.

We observe that the two density arguments (a) and (c) above, make the kernel of (A2) approach $K_{xc}\{y,n(\frac{1}{2}r')\}$, if r is fixed and $r'\gg r$. As the densities $n(\frac{1}{2}r')$ decays exponentially with r', so does the corresponding $k_F(n)$ and therefore yk_F approaches zero exponentially. From (A3) it is then clear that the behavior of $K_{xc}\{y,n\}$ as $y\to 0$ will govern the convergence of ΔE_{xc} in these cases.

The Fourier transform of the kernel is

$$K_{xc}(\vec{r},n)=\frac{1}{(2\pi)^3}\int d^3k\,K_{xc}(\vec{k},n)e^{i\vec{k}\cdot\vec{r}}, \tag{A4}$$

with $K_{xc}(\vec{k},n)$ according to Eq. (29). With the common definition of the dielectric function $\epsilon(k,n)$ in terms of the local-field correction $G(k,n)$[39]

$$\epsilon(k,n)=1-\frac{v(k)\chi_0(k,n)}{1+G(k,n)v(k)\chi_0(k,n)}, \tag{A5}$$

where $v(k)=4\pi e^2/k^2$ and $\chi_0(k,n)$ is the polarizability of the noninteracting electron gas, one obtains

$$K_{xc}(k,n)=-v(k)G(k,n). \tag{A6}$$

According to Eqs. (A4) and (A6) the small-r behavior of $K_{xc}(\vec{r},n)$ relates to the large-k behavior of $G(k,n)$. It is known that $G(k,n)$ goes to a constant value as k approaches infinity. This constant is $\frac{1}{3}$ in the Hartree-Fock approximation,[13] and it is estimated to be in the range from $\frac{1}{3}$ to $\frac{2}{3}$ when correlation is included.[40] As the behavior of $K_{xc}(k,n)$ for large $k/k_F(n)$ dominates the form of $K_{xc}(\vec{r},n)$ for small values $rk_F(n)$, we get

$$K_{xc}(\vec{r},n)\xrightarrow[rk_F(n)\to 0]{}-G(k\to\infty,n)(e^2/r). \tag{A7}$$

We may now return to (A2) and perform the y integration, which for large values of r' attains the value

$$-2rn(r)^2e^2G(k\to\infty,n). \tag{A8}$$

As this quantity is independent of r', it is obvious that the r' integral is divergent, and therefore ΔE_{xc} goes towards plus infinity. This result is in disagreement with a numerical calculation by Sham,[14] who has reported a finite result for ΔE_{xc}.

If, on the other hand, one uses the density argument (b), i.e., $\frac{1}{2}[n(\vec{r})+n(\vec{r}')]$, which approaches a constant value for growing r' but fixed r, yk_F goes towards infinity instead of zero. In this limit K_{xc} behaves at worst as

$$K_{xc}(y,n)\underset{yk_F\to\infty}{\sim}[\sin(2k_Fy+\Phi)]/y^3 \tag{A9}$$

due to the logarithmic singularity of $K_{xc}(k,n)$ for $k=2k_F$, present at least in the approximate solution of Geldart and Taylor.[13] This decay is sufficiently rapid to ensure that the integral (A2) is convergent, as shown below. Because the density is exponentially decaying, the factor $[n(r)-n(r')]^2$ will cut off all contributions from large values of r. A possible divergence would therefore appear only if the integrand decays too slowly for fixed r but large and growing r'. First, we therefore consider the y integral. A partial integration gives that

$$\int_{|r'-r|}^{r'+r} y\,dy\,K_{xc}(y,n)\sim\left[-\frac{\cos(2k_Fy+\Phi)}{y^2}\right]_{|r'-r|}^{r'+r}+O(r'^{-3}). \tag{A10}$$

From a similar partial integration over r', it follows that the integral over r' between a large value R' and infinity goes as $1/R'$. Therefore no divergence occurs in the limit $r'\to\infty$ and the exchange-correlation energy is finite for the density argument (b).

APPENDIX B

The second-order expansion Eq. (3) for the XC energy functional involves a kernel $K_{xc}(\vec{r}-\vec{r}',n)$ with an incompletely specified density argument n. In this appendix we will show that the choice (a) $n=n(\frac{1}{2}(\vec{r}+\vec{r}'))$ leads to a divergent result for the surface energy when this expansion of E_{xc} is applied to the jellium model of a metal surface.[28] We will also show that the choice (b) $n=\frac{1}{2}[n(\vec{r})+n(\vec{r}')]$ gives a convergent result in the same situation.

The electron density $n(z)$ of this model depends only on the distance z perpendicular to the surface. On the vacuum side ($z>0$) of the surface the den-

sity decays exponentially, while inside the surface it has a Friedel oscillation decaying as $1/z^2$, i.e., the density approaches a constant value n.

The surface energy is defined as one-half of the energy difference between two separated half-infinite systems and an infinite system. For an infinite metal in the jellium model, the density is constant, and the second-order term in Eq. (3) is zero. The second-order contribution to the surface energy is therefore

$$\Delta E_{\rm XC}^{\rm surf} = -\frac{1}{4}\int_{-\infty}^{\infty} dz \int_{-\infty}^{\infty} dz' [n(z)-n(z')]^2 \times \int d^2\rho \int d^2\rho' K_{\rm XC}(|\vec{r}-\vec{r}'|, n), \quad \text{(B1)}$$

where ρ is the coordinate parallel to the surface. As the integrand depends on $\vec{\rho}$ and $\vec{\rho}'$ only through the difference $\vec{\rho}-\vec{\rho}'$, the surface energy per unit area is

$$\frac{1}{A}\Delta E_{\rm XC}^{\rm surf} = -\frac{\pi}{2}\int_{-\infty}^{\infty} dz' [n(z)-n(z')]^2 \times \int_0^{\infty} \rho d\rho K_{\rm XC}([\rho^2+(z-z')^2]^{1/2}, n). \quad \text{(B2)}$$

If we now invoke the approximation Eq. (A3), i.e.,

$$K_{\rm XC}(r,n) \simeq k_F(n) f(r k_F(n))$$

and make the variable substitutions $R=\frac{1}{2}(z+z')$, $r=z-z'$ and $y^2=\rho^2+(z-z')^2$, Eq. (B2) takes the form

$$\frac{1}{A}\Delta E_{\rm XC}^{\rm surf} = -\pi \int_{-\infty}^{\infty} dR \int_0^{\infty} dr\, [n(R+\tfrac{1}{2}r)-n(R-\tfrac{1}{2}r)]^2 \frac{1}{k_F} \times \int_{rk_F}^{\infty} y\, dy f(y). \quad \text{(B3)}$$

When determining the convergence properties of Eq. (B3) we shall adopt the strategy of performing the integration over the variables r and R in a number of separate regions of the (r,R) plane, chosen so that in each region the integrand reduces to a simple form.

We shall first treat the integration region $R > -a$ and $\frac{1}{2}r > |R| + a$, where a is chosen so that $n(a)/n_0 \ll 1$ and $|n(-a)-n_0|/n_0 \ll 1$. Then the density difference in the square brackets of (B3) is close to $-n_0$ and it can be brought outside the r integral. Reversing the order of the r and y integrations one gets

$$I(R) \equiv \int_{2(|R|+a)}^{\infty} dr \int_{rk_F}^{\infty} y\, dy f(y) k_F^{-1}(n) = k_F^{-1}(n) \int_{2(|R|+a)k_F}^{\infty} y\, dy \left(\frac{y}{k_F} - 2(|R|+a)\right) f(y). \quad \text{(B4)}$$

The choice (a) gives the density argument $n(R)$, which goes exponentially to zero when R grows. Thus we get

$$I(R) \underset{R\to\infty}{\longrightarrow} k_F^{-2}(n(R)) \int_0^{\infty} y^2\, dy f(y). \quad \text{(B5)}$$

The integration over R is thus strongly *divergent*. If instead the form (b) is applied, the density argument is $\frac{1}{2}n_0$ and k_F is a constant. Then the lower limit of integration in Eq. (B4) grows with R and $f(y)$ may be replaced by the limiting form $f(y) = \sin(2y+\phi)/y^3$, valid for large y (cf. Eq. A9). Now it requires only two succesive partial integrations of Eq. (B4) (or, indeed, of Eq. 13 directly) to verify that to leading order $I(R) \propto R^{-2}$, which makes the integration over R *convergent* in this domain of the (r,R) plane.

We next consider the region where $R < -a$ and $\frac{1}{2}r > |R| + a$. Here it is still true that $R + r/a > a$ and $\frac{1}{2}R - r < -a$, making the density difference in Eq. (B3) close to $-n_0$. Furthermore, *both* choices (a) and (b) yield constant density arguments, viz., n_0 and $\frac{1}{2}n_0$. The arguments given above then apply again and *no divergencies* occur.

In the domain where $R > a$ and $R - a < \frac{1}{2}r < R + a$, the inequalities $R + \frac{1}{2}r > a$ and $-a < (R - \frac{1}{2}r) < a$ also holds, and therefore the density difference $n(R+\frac{1}{2}r) - n(R-\frac{1}{2}r)$ is of order n_0. For the density argument (a), $rk_F(n)$ will approach zero as R grows. The r integration in Eq. (B3) is then trivial, the result being of order

$$4an_0^2 k_F^{-1}(n(R)) \int_0^{\infty} y\, dy f(y).$$

The remaining integration over R obviously *diverges*. With the choice (b) the density argument will again be constant, of order n_0, and it is easy to verify that the contribution to Eq. (B3) from this region is now *convergent*.

In the domain where $R > a$ and $0 < \frac{1}{2}r < R - a$, we use again that for the density argument (a) $rk_F(n)$ approaches zero for large R. Assuming that the density for large distances z from the surface has the behavior $n(a)e^{[-\lambda(z-a)]}$ we find that the R integrand grows as

$$n(a)^2 [\lambda k_F(n(R))]^{-1} \int_0^{\infty} y\, dy f(y)$$

which makes the R integral *diverging*. For the density argument (b) we use the estimate

$$\left| \int_{rk_F}^{\infty} y\, dy f(y) \right| \le \frac{b}{(rk_F)^2 + d}, \quad \text{(B6)}$$

which is based on the facts that (B6) should be finite for $r=0$ and decay as $(rk_F)^{-2}$ for large rk_F. Using this estimate we have shown that (b) makes the R integral *convergent* in this region.

There are two domains still to be considered, first where $R<-a$ and $|R|-a<\frac{1}{2}r<|R|+a$. Both prescriptions for choosing density argument lead to $n=n_0$, as $R-\frac{1}{2}r<-a$ and $R+\frac{1}{2}r<-a$. The integral therefore *converges* due to arguments given above.

In the final region $R<-a$ and $0<\frac{1}{2}r<|R|-a$ again *both* (a) and (b) give a constant density argument. Due to Friedel oscillations the density difference does not decay exponentially, but

$$[n(R+\tfrac{1}{2}r)-n(R-\tfrac{1}{2}r)]^2<\frac{C(n_0)}{(|R|-\frac{1}{2}r)^4}. \tag{B7}$$

Using B6 we find that this is sufficient to ensure *convergence* also in this region.

Before we conclude that the density argument (a) gives a divergent contribution, we have to exclude the possibility that the divergencies we have found in two regions of the (r,R) plane cancel. It suffices to show that they have the same sign. This will be the case if the integrals $I_1=\int_0^\infty y^2\,dy\,f(y)$ and $I_2=\int_0^\infty y^2\,dy\,f(y)$ have the same sign. After observing that $I_1\propto f(k)$ and $I_2\propto\int_0^\infty dk\,f(k)$, where $f(k)$ is the Fourier transform of $f(y)$, we may use the numerical values of $f(k)$ due to Geldart and Taylor[13] to convince ourselves that I_1 and I_2 indeed have the same sign.

To summarize, we have shown that use of the density argument (a), $n(\frac{1}{2}(\vec{r}+\vec{r}'))$, gives a divergent surface energy, while the argument (b), $\frac{1}{2}[n(\vec{r})+n(\vec{r}')]$, gives a finite result.

APPENDIX C

This appendix is devoted to a discussion of the differential equation in Eq. (30)

$$[w(k,r_s)]^2+2A(r_s)w(k,r_s)\left(1-\tfrac{1}{3}r_s\frac{\partial w(k,r_s)}{\partial r_s}\right)$$

$$-[1+2A(r_s)]f(k,r_s)=0. \tag{C1}$$

In Sec. III the normalization condition

$$w(k=0,r_s)=1 \tag{C2}$$

was imposed. This condition has to be transformed to a boundary condition for the differential equation Eq. (C1). This is done by noting that the only characteristic wave vector involved in the problem is $k_F=1/\alpha r_s$. For $k/k_F=k\alpha r_s\ll 1$, $w(k,r_s)$ should therefore approach the limit $w(k=0,r_s)$. In particular, for an arbitrary value of k

$$\lim_{r_s\to 0} w(k,r_s)=w(k=0,r_s)=1. \tag{C3}$$

This result supplies the desired boundary condition for Eq. (C1). The differential equation is nonlinear and it is singular in the sense that the coefficient in front of the derivative vanishes for $r_s=0$. It has therefore unusual features and a careful investigation of its properties is necessary.

In Fig. 17 the (w,r_s) plane is shown. The two full curves mark where $\partial w/\partial r_s$ changes sign according to Eq. (C1). We shall first consider the integration of Eq. (C1) in the positive r_s direction, using Eq. (C3) as an initial condition. The gross features of the solution can be understood by considering the sign of $\partial w/\partial r_s$. If, during the integration the solution gets below the lowest full curve the derivative becomes negative and the solution has a tendency to go towards the r_s axis. At the r_s axis it becomes nonanalytic because of the singularity in the differential equation for $w=0$. If the solution gets above the lowest full curve (but below the upper one) the derivative becomes positive and the solution tends to join the upper full curve. Thus the lower curve repels the solution and the upper one attracts it. We now reverse this procedure and integrate in the negative r_s direction starting at some initial value of $w(k,r_{s0})$ for a large r_{s0}. Now the full curves have the opposite properties and the solution aims at the lower one (provided that it is not above the upper curve). In particular, as $r_s\to 0$ the singularity in Eq. (18) forces the solution to satisfy the condition (C3), i.e., $w(k,r_s=0)=1$. This is true for a large class of solutions which start sufficiently far below the upper full curve. This indicates that the boundary

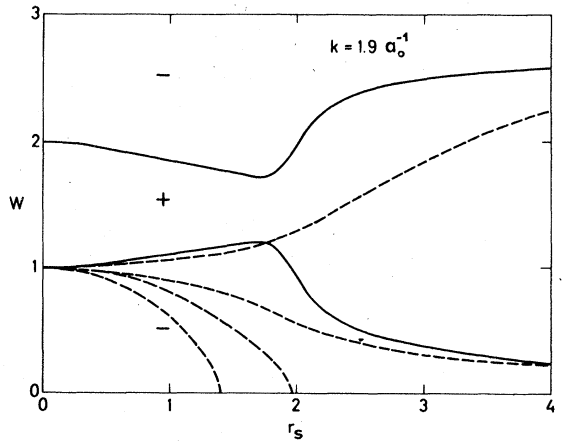

FIG. 17. (w,r_s) plane for $k=1.9a_0^{-1}$ of Eq. (C1). The full curves show where $\partial w/\partial r_s$ changes sign and its sign is indicated by the plus and minus signs in the figure. Depending on the slope of the solution at $r_s=0$ a number of different solutions are obtained. These solutions are shown schematically in this figure.

condition in Eq. (C3) does not define a unique solution. This will now be proven. Let $w_0(k,r_s)$ be a solution to the differential equation Eq. (C1) satisfying (C3). Assume further that

$$w(k,r_s) \equiv w_0(k,r_s) + w_1(k,r_s)$$

also satisfies Eqs. (C1) and (C3). Eq. (C1) may then be rewritten as

$$2w_0(k,r_s)w_1(k,r_s) + w_1(k,r_s)^2 + 2A(r_s)w_1(k,r_s)\left[1 - \frac{1}{3}r_s\left(\frac{\partial w_0(k,r_s)}{\partial r_s} + \frac{\partial w_1(k,r_s)}{\partial r_s}\right)\right] - \tfrac{2}{3}A(r_s)w_0(k,r_s)r_s\frac{\partial w_1(k,r_s)}{\partial r_s} = 0 . \tag{C4}$$

It is now assumed that $w_1(k,r_s)$ has a power expansion

$$w_1(k,r_s) = \sum_{\nu=1}^{\infty} a_\nu r_s^{\nu\gamma} , \tag{C5}$$

with $\gamma > 0$. Inserting (C5) into (C4) reveals that a_1 can have any value provided

$$\gamma \equiv 3[1/A(0) + 1] = 1 .$$

This means that there are an infinite number of solutions satisfying Eqs. (C1) and (C3) and an additional condition is required. In connection with Fig. 17 we observed that the solutions starting at $w(k,0) = 1$ tends to go towards either $2|A(r_s)|$ or the r_s axis. In the latter case the solution is undefined for large r_s and not acceptable. Let us instead assume that

$$\lim_{r_s \to \infty} w(k,r_s) = 2|A(r_s)| .$$

This corresponds to

$$\lim_{k \to \infty} w(k,r_s) = 2|A(r_s)|$$

according to arguments of the same type as those leading to Eq. (C3). In this case the real-space weight function takes the form

$$w(r,r_s) = 2|A(r_s)|\delta(r) + \bar{w}(r,r_s) ,$$

where $w(r,r_s)$ integrates up to $1 - 2|A(r_s)| < 0$. Such a form for w is unphysical. From Fig. 17 it follows that the only remaining possibility is that $w(k,r_s)$ goes towards zero,

$$\lim_{r_s \to \infty} w(k,r_s) = 0 , \tag{C6}$$

which we impose as a second boundary condition.

That this condition defines a unique solution can be seen in the following way. A coordinate transformation $x = 1/r_s$ is made. The new differential equation resulting from this transformation has exactly the same singularity at $x = 0$ as the old one has for $r_s = 0$ and there will be an infinite number of solutions starting at $2|A(r_s)|$. However, there is just one solution starting from zero. To prove this, assume that

$$w(k,x) = w_0(k,x) + w_1(k,x) ,$$

$$w_1(k,x) = \sum_{\nu=1}^{\infty} a_\nu x^{\nu\gamma} , \tag{C7}$$

and consider the equation for $w_1(k,x)$, which is similar to Eq. (C4). We find that the terms which are nonlinear in w do not contribute to lowest order in x, and the contribution from the linear term cannot be cancelled by any other term if $w_1(k,x) \neq 0$. The difference compared to the case when the solution starts from $2|A|$ is that $w(k,x=0) = 2|A|$ allows the mixed term $w_0(k,x)w_1(k,x)$ to contribute to lowest order in x.

We conclude, then, that the boundary conditions $w(k,0) = 1$ and $\lim_{r_s \to \infty} w(k,r_s) = 0$ uniquely define a solution to the differential equation of Eq. (C1).

In the numerical calculations we have used data from Ref. 19 for $\epsilon_{xc}(r_s)$ to calculate $A(r_s)$. [$A(r_s)$ is defined below Eq. (30)]. Data for $f(k,r_s)$ have been obtained from Ref. 13. There data is given for the range $1 < r_s < 6$. For $r_s \gg 6$ we utilize the fact that

$$\bar{f}(q,r_s) = f(qk_F,r_s)$$

has a weak r_s dependence if the dimensionless variable q is kept fixed. We have used two different procedures. First $\bar{f}(q,r_s)$ was assumed r_s independent for $r_s > 6$ and then a linear extrapolation was used in the range $6 < r_s < 9$ together with the assumption that $f(q,r_s)$ is constant for $r_s > 9$. For $r_s < 6$ these two approaches gave essentially the same result for $w(k,r_s)$. The numerical data for $w(k,r_s)$ presented are calculated according to the latter scheme. For $r_s = 0$ the correlation effects are negligible and we can use the data only including exchange effects as will be discussed below. In practice the integration of Eq. (C1) is performed by starting at some large value of r_s so that $k > k_F(r_s) \equiv 1/\alpha r_s$. Then $w(k,r_s) \ll 1$ and Eq. (C1) reduces to a linear algebraic equation, which provides a starting value. Eq. (C1) is then integrated in the negative r_s direction.

It is convenient to present data for $\tilde{w}(q,r_s) \equiv w(qk_F,r_s)$ as $\tilde{w}(q,r_s)$ has a weak r_s dependence. The numerical results are shown in Table I and

Fig. 9.

In the case when only exchange effects are included, $A(r_s)$ becomes r_s independent $[A(r_s)\equiv 1.5]$. For the function $f(k,r_s)$ we then use the same form as Sham.[14] The polarizability defined by

$$\epsilon(k)=1-v(k)\chi(k)$$

is expanded in powers of e^2: $\chi(k)=\chi_0+\chi_1+\cdots$. The higher-order terms are approximated by geometric progression starting with the first two terms, which are obtained from a calculation of Geldart and Taylor.[13] The function $\tilde{f}(q,r_s)$ is then independent of r_s. Expressed in terms of the dimensionless variable q, Eq. (C1) thus also becomes r_s independent. Therefore there exists a solution $\tilde{w}_{ex}(q)$ which has no r_s dependence. In the limit when r_s tends to zero this solution agrees with the solution to the differential equation that includes correlation effects, as correlation effects are negligible in this limit.

APPENDIX D

We will here derive simplified expressions for the XC potentials for the metal surface system. Starting with the WD approximation, we may according to Eqs. (40) and (41) express v_{XC}^{WD} as a sum of three terms.

$$v_{XC}^{WD}(\vec{r})=v_1(\vec{r})+v_2(\vec{r})+v_3(\vec{r})\,. \tag{D1}$$

In Eq. (40) $\vec{r}'$ has to be inside the metal to give a contribution to the integral. It is therefore reasonable in the second term $v_2(\vec{r})$ to replace the density argument $\bar{n}(\vec{r}')$ of G^h with the bulk density n_0

$$v_2(\vec{r})\simeq\frac{1}{2}\int d^3r'\,n(\vec{r}')v(\vec{r}-\vec{r}')G^h(\vec{r}-\vec{r}';n_0) \tag{D2}$$

The same argument may be applied to $v_3(\vec{r})$, which may then be written as

$$v_3(\vec{r})=-\int d^3r'\,n(\vec{r}')G^h(\vec{r}-\vec{r}';n_0)F(\vec{r}')\,, \tag{D3}$$

where

$$F(\vec{r}')=\frac{1}{2}\int d^3r''n(\vec{r}'')v(\vec{r}'-\vec{r}'')\frac{\partial G^h(\vec{r}''-\vec{r}';n_0)}{\partial n_0}\times\left(\int d^3x\,n(\vec{x})\frac{\partial G^h(\vec{x}-\vec{r}';n_0)}{\partial n_0}\right)^{-1}. \tag{D4}$$

The denominator D of Eq. (E3) may be written

$$D=\alpha_1 n_0\int d^3x\frac{\partial G^h(\vec{x}-\vec{r}';n_0)}{\partial n_0}=\alpha_1 n_0\frac{d}{dn_0}\left(-\frac{1}{n_0}\right)=\frac{\alpha_1}{n_0}, \tag{D5}$$

where the sum rule Eq. (36) applied to a homogeneous system has been used. Clearly, if $\vec{r}'$ is deep inside the metal α_1 is unity and if $\vec{r}'$ is at the surface $\alpha_1\simeq 0.5$. Similarily, the numerator of Eq. (D4) can be written

$$N=\alpha_2 n_0\frac{1}{2}\int d^3r''\,v(\vec{r}'-\vec{r}'')\frac{d}{dn_0}G^h(\vec{r}''-\vec{r}';n_0)=\alpha_2 n_0\frac{d}{dn_0}\left(\frac{1}{n_0}\epsilon_{XC}^{bulk}\right)=\alpha_2\left(\frac{1}{n_0}\right)\left(-\epsilon_{XC}^{bulk}+n_0\frac{d}{dn_0}\epsilon_{XC}^{bulk}\right), \tag{D6}$$

where again $0.5\lesssim\alpha_2\lesssim 1$, as $\vec{r}'$ has to be inside the metal. Now, as

$$F(r')=\left(\frac{\alpha_2}{\alpha_1}\right)\left(-\epsilon_{XC}^{bulk}(n_0)+n_0\frac{d}{dn_0}\epsilon_{XC}^{bulk}(n_0)\right), \tag{D7}$$

where we expect α_2/α_1 to be close to unity for all values of $\vec{r}'$. A reasonable approximation to $v_3(\vec{r})$ is therefore

$$v_3(\vec{r})=-\int d^3r'\,n(\vec{r}')G(\vec{r}-\vec{r}';n_0)\times\left(-\epsilon_{XC}^{bulk}(n_0)+n_0\frac{d}{dn_0}\epsilon_{XC}^{bulk}(n_0)\right). \tag{D8}$$

For $\vec{r}'$ deep inside the metal this approximate form of the potential (D1) tends to the correct limit $(d/dn_0)[n_0\epsilon_{XC}^{bulk}(n_0)]$.

In the AD approximation the XC potential is given by Eqs. (33) and (34). As in the case of the WD approximation we may replace the density argument $\bar{n}(\vec{r}')$ with the bulk density n_0. This is a good approximation, since $\vec{r}'$ has to be inside the metal to contribute to the integral in Eq. (33). Furthermore the denominator in Eq. (34) may be written $[\bar{n}(\vec{r}')-n_0]$

$$D=1-n_0\frac{d}{dn_0}\left(\alpha(n_0)\int d^3r''\,w(\vec{r}'-\vec{r}'';n_0)\right)=1-n_0\frac{d\alpha(n_0)}{dn_0}. \tag{D9}$$

In the SCIBM model, $\alpha(n_0)=1$ if $\vec{r}'$ is deep inside the metal, and $\alpha(n_0)=0.5$ if $\vec{r}'$ is exactly at the surface (thus independent of the density n_0). It is therefore reasonable to assume that α is only weakly density dependent ant let D be unity. Thus the approximate form of v_{XC}^{AD} is

$$v_{XC}^{AD}(\vec{r})\simeq\epsilon_{XC}^{AD}(\vec{r})+\frac{d\epsilon_{XC}^{bulk}(n_0)}{dn_0}\times\int d^3r'\,n(\vec{r})w(\vec{r}-\vec{r}';n_0) \tag{D10}$$

which again tends to the correct limit far inside the metal.

APPENDIX E

This Appendix contains a discussion of the XC part of the surface energy, σ_{XC}^{AD}, of a jellium surface in the IBM. We shall find that σ_{XC}^{AD} has unreasonably large contributions from deep inside the metal (large negative z value). This result is a deficiency of the AD approximation and independent of the IBM *per se*. The surface energy in the AD approximation is given by[28]

$$\sigma_{XC}^{AD}=\int_{-\infty}^{\infty} dz\, n(z)[\epsilon_{XC}(\bar{n}(z))-\epsilon_{XC}^{bulk}(n_0)]\,, \tag{E1}$$

where $\bar{n}(z)$ is given by Eq. (21). The convergence properties of the integral are best studied by adding and subtracting terms to Eq. (E1) to get

$$\sigma_{XC}^{AD}=n_0\frac{d\epsilon_{xc}}{dn_0}\left(\int_{-\infty}^{0} dz[\bar{n}_0(z)-n_0]+\int_{-\infty}^{0} dz[\bar{n}(z)-\bar{n}_0(z)]\right)$$
$$+\int_{-\infty}^{0} dz\, n_0\left(\epsilon_{xc}(\bar{n}(z))-\epsilon_{xc}(n_0)-[\bar{n}(z)-n_0]\frac{d\epsilon_{xc}}{dn_0}\right)+\int_{-\infty}^{\infty} dz[n(z)-n_0\theta(-z)]\,[\epsilon_{xc}(\bar{n}(z))-\epsilon_{xc}(n_0)]\,, \tag{E2}$$

where we have introduced

$$\bar{n}_0(z)=\int d^3r'\, n(\vec{r}')w(\vec{r}-\vec{r}';n_0)\,. \tag{E3}$$

In all but the first integral in Eq. (E2) the density variation enters only in second order and convergence is ensured. We shall therefore only consider the integral

$$I=n_0^{-1}\int_{-\infty}^{0} dz[\bar{n}_0(z)-n_0]\,, \tag{E4}$$

whose convergence depends on the behavior of the integrand as $z\to-\infty$!

In combining Eqs. (E3) and (E4) it is convenient to express $n(z)$ and $w(\vec{r})$ as Fourier integrals. The Fourier transform of $n(z)$ [Eq. (52)] is readily calculated as

$$n(q)/n_0=\pi\delta(q)-(3\pi/8k_F)(1-q^2/4k_F^2)(2k_F-|q|)$$
$$+i(P/q-3q/8k_F^2)\,, \tag{E5}$$

and the integrand of Eq. (E4) is

$$\bar{n}_0(z)-n_0=-\frac{3n_0}{8}\int_0^2 dq\, w(q,n_0)(1-\tfrac{1}{4}q^2\cos(qz)$$
$$+\frac{n_0}{\pi}\int_0^{\infty}\frac{dq}{q}\sin(qz)[1-w(q,n_0)f(q)]\,, \tag{E6}$$

TABLE VII. Sensitivity of Eq. (E2) for σ_{XC}^{AD} at $r_s=2$ to a low cutoff q_c introduced into the integral in Eq. (E9). The local-density approximation gives $\sigma_{XC}^{LD}=1350$ ergs/cm^{-2}.

q_c (k_F)	$1/q_c$ (k_F^{-1})	σ_{XC}^{AD} (ergs/cm^2)
0.05	20	1760
0.10	10	1580
0.15	6.7	1450
0.20	5.0	1360
0.25	4.0	1280
0.30	3.3	1220
0.35	2.9	1160

where

$$f(q)=1-\frac{3q^2}{8}\left(1-\frac{q^2/4-1}{q}\ln[(q+2)/(q-2)]\right)\,. \tag{E7}$$

The integration over z may be performed by introducing a convergence factor $\exp(\alpha z)$ in the standard manner. We find that

$$\lim_{\alpha\to0}\int_0^{\infty} dz\cos(qz)\exp(\alpha z)=\pi\delta(z)\,,$$

$$\lim_{\alpha\to0}\int_0^{\sigma} dz\sin(qz)\exp(\alpha z)=-\frac{P}{q}\,. \tag{E8}$$

On combining Eqs. (E4), (E6) and (E8) we get

$$I=-\frac{3\pi}{16}-\pi^{-1}\int_0^{\infty}\frac{dq}{q^2}[1-w(q,n_0)f(q)]\,. \tag{E9}$$

Now as $f(q)$ tends to unity, as q tends to zero, $w(q)$ must tend to unity at least as $q^{1+\alpha}$ for the integral in Eq. (E9) to be finite. The function $w(q)$ was obtained by numerically solving a differential equation (see Appendix C) and therefore we have no analytical expression for $w(q)$ at small-q values. From the tabulated values (Table I) or from Fig. 9 it is clear, however, that $w(q)-1$ rather than being quadratic in q seems to be linear in q for small-q values. If $w(q)$ indeed had a linear term in q at small q, then Eq. (E2) would diverge. Even if for very-small-q values the linear term would no longer be there, the contribution from the small-q region (corresponding to the large-$|z|$ region) would be unreasonably large, as can be seen from Table VII where a cutoff q_c has been introduced into Eq. (E9). The accuracy in our numerical solution for $w(q)$ does not permit a definite answer to the question whether σ_{XC}^{AD} diverges, or if it is just too large.

*Present address: Physics Dept., Indiana, Univ., Bloomington, Ind. 47401.
†Present address: Institute of Theoretical Physics, Chalmers University of Technology, S-41296 Göteborg, Sweden.

[1]W. Kohn and L. J. Sham, Phys. Rev. 140, A1133 (1965).
[2]P. Hohenberg and W. Kohn, Phys. Rev. 136, B864 (1964).
[3]See, e.g., O. Gunnarsson and B. I. Lundqvist, Phys. Rev. B 13, 4274 (1976), and references therein.
[4]B. Y. Tong and L. J. Sham, Phys. Rev. 144, 1 (1966).
[5]N. D. Lang and W. Kohn, Phys. Rev. B 1, 4555 (1970); 3, 1215 (1971).
[6]F. Herman, J. P. van Dyke, and I. B. Ortenberger, Phys. Rev. Lett. 22, 807 (1969).
[7]D. J. W. Geldart, M. Rasolt, and R. Taylor, Solid State Commun. 10, 279 (1972).
[8]O. Gunnarsson, B. I. Lundqvist, and J. W. Wilkins, Phys. Rev. B 10, 1319 (1974).
[9]K. H. Schwartz, Chem. Phys. 7, 94 (1975).
[10]J. H. Rose Jr., H. B. Shore, D. J. W. Geldart, and M. Rasolt, Solid State Commun. 19, 619 (1976).
[11]K. H. Lau and W. Kohn, J. Phys. Chem. Solids 37, 99 (1976).
[12]J. H. Rose Jr. and H. B. Shore, Solid State Commun. 17, 1327 (1975).
[13]D. J. W. Geldart and R. Taylor, Can. J. Phys. 48, 155 (1970); 48, 167 (1970).
[14]L. J. Sham, Phys. Rev. B 7, 4357 (1973).
[15]J. P. Perdew and D. C. Langreth, Solid State Commun. 17, 1425 (1975).
[16]O. Gunnarsson, M. Jonson, and B. I. Lundqvist, Phys. Lett. 59A, 177 (1976).
[17]O. Gunnarsson, M. Jonson, and B. I. Lundqvist, Solid State Commun. 24, 765 (1977).
[18]J. A. Alonso and L. A. Girifalco, Solid State Commun. 24, 135 (1977); Phys. Rev. B 17, 3735 (1978).
[19]See, e.g, P. Vashishta and K. S. Singwi, Phys. Rev. B 6, 875 (1972).
[20]L. Hedin, in *Computational Solid State Physics*, edited by F. Herman, N. W. Dalton, and T. R. Koehler (Plenum, New York, 1972), p. 233.
[21]O. Gunnarsson, J. Appl. Phys. 49, 1399 (1978).
[22]B. Y. Tong, Phys. Rev. A 4, 1375 (1971).
[23]E. Clementi, IBM J. Res. Dev. 9, 2 (1965).
[24]E. Clementi, J. Chem. Phys. 38, 2248 (1963); 39, 175 (1963).
[25]H. B. Shore, J. H. Rose, and E. Zaremba, Phys. Rev. B 15, 2858 (1977).
[26]P. Grimstrup (private communication).
[27]This procedure has been suggested independently by P. Grimstrup (private communication) and U. von Barth (private communication).
[28]N. D. Lang, in *Solid State Physics*, edited by H. E. Ehrenreich, F. Seitz, and D. Turnbull (Academic, New York, 1973), Vol. 28.
[29]H. Hjelmberg, O. Gunnarsson, and B. I. Lundqvist, Surf. Sci. 68, 158 (1977); N. D. Lang and A. R. Williams, Phys. Rev. Lett. 37, 212 (1976).
[30]See, for instance, D. M. Newns, Phys. Rev. B 1, 3304 (1970).
[31]N. D. Lang and W. Kohn, Phys. Rev. B 1, 4555 (1970).
[32]This is equivalent to the "quasi-classical IBM" discussed by D. E. Beck, V. Celli, G. LoVecchio, and A. Magnaterra [Nuovo Cimento B68, 230 (1970)].
[33]See p. 75 of Ref. 34.
[34]D. Pines, in *Elementary Excitations in Solids* (Benjamin, New York, 1964), p. 94.
[35]J. E. Inglesfield and E. Wikborg, Solid State Commun. 16, 335 (1975).
[36]D. C. Langreth and J. P. Perdew, Phys. Rev. B 15, 2884 (1977).
[37]K. S. Singwi, A. Sjölander, M. P. Tosi, and R. H. Land, Phys. Rev. B 1, 1044 (1970).
[38]A nonlocal exchange-energy functional identical to the WD approximation has independently been suggested by J. Alonso and L. A. Girifalco [Solid State Commun. 24, 135 (1977)]; and unpublished.
[39]L. Hedin and S. Lundqvist, Solid State Phys. 23, 1 (1969).
[40]G. Niklasson, Phys. Rev. B 10, 3058 (1974).